Award Number: DAMD17-01-1-0366

TITLE: Maximizing Immune Response to Carbohydrate Antigens on Breast Tumors

PRINCIPAL INVESTIGATOR: Thomas Kieber-Emmons, Ph.D.

CONTRACTING ORGANIZATION: University of Arkansas for Medical Science
Little Rock, Arkansas 72205

REPORT DATE: August 2004

TYPE OF REPORT: Annual

PREPARED FOR: U.S. Army Medical Research and Materiel Command
Fort Detrick, Maryland 21702-5012

DISTRIBUTION STATEMENT: Approved for Public Release;
Distribution Unlimited

The views, opinions and/or findings contained in this report are those of the author(s) and should not be construed as an official Department of the Army position, policy or decision unless so designated by other documentation.

20050715 118

REPORT DOCUMENTATION PAGE

Form Approved
OMB No. 074-0188

Public reporting burden for this collection of information is estimated to average 1 hour per response, including the time for reviewing instructions, searching existing data sources, gathering and maintaining the data needed, and completing and reviewing this collection of information. Send comments regarding this burden estimate or any other aspect of this collection of information, including suggestions for reducing this burden to Washington Headquarters Services, Directorate for Information Operations and Reports, 1215 Jefferson Davis Highway, Suite 1204, Arlington, VA 22202-4302, and to the Office of Management and Budget, Paperwork Reduction Project (0704-0188), Washington, DC 20503

1. AGENCY USE ONLY (Leave blank)	2. REPORT DATE	3. REPORT TYPE AND DATES COVERED
	August 2004	Annual (15 Jul 2003 - 14 Jul 2004)

4. TITLE AND SUBTITLE
Maximizing Immune Response to Carbohydrate Antigens on Breast Tumors

5. FUNDING NUMBERS
DAMD17-01-1-0366

6. AUTHOR(S)
Thomas Kieber-Emmons, Ph.D.

7. PERFORMING ORGANIZATION NAME(S) AND ADDRESS(ES)
University of Arkansas for Medical Sciences
Little Rock, Arkansas 72205

E-Mail: tke@uams.edu

8. PERFORMING ORGANIZATION REPORT NUMBER

9. SPONSORING / MONITORING AGENCY NAME(S) AND ADDRESS(ES)
U.S. Army Medical Research and Materiel Command
Fort Detrick, Maryland 21702-5012

10. SPONSORING / MONITORING AGENCY REPORT NUMBER

11. SUPPLEMENTARY NOTES

12a. DISTRIBUTION / AVAILABILITY STATEMENT
Approved for Public Release; Distribution Unlimited

12b. DISTRIBUTION CODE

13. ABSTRACT (Maximum 200 Words)

Tumor antigens are autologous antigens and thus are weakly immunogenic. Unresponsiveness appears to be related to suppression of antigen specific helper T cell function which can be overcome by providing heterologous help. Carbohydrates are richly expressed on the surface of many cancers, at frequencies higher than oncogene products. Consequently, tumor associated carbohydrate antigens, are in principle, excellent targets for immunotherapy. However, carbohydrates are generally poor at eliciting effective antibody responses and rarely provide target epitopes for CTL because of their T cell-independent nature. The major objective of this application is to examine ways to maximize the tumor-protective immunity directed to carbohydrate antigens expressed on breast tumors. Towards this end we are developing peptide mimotopes of tumor associated carbohydrate antigens as they are T cell dependent antigens. In our progress to date we have shown that 1.) We observed that transfection with Fut 3 changes the expression profile of E selectin reactivity. 2) We defined potential peptide mimotopes for targeting 4T1 cells in vivo. 3) We observed that immunization with DNA induced IgM antibodies reactive with 4T1 cells. 4) We observed that DNA administration of 4T1-tumor bearing animal temporarily reduces the burden of tumor. 5) DNA administration of the 107 peptide significantly increases survival rate of animals. 6) We observed that administration of 107 DNA inhibits liver metastases.

14. SUBJECT TERMS
Cellular (T-cell) immunology, tumor immunology, DNA immunology, IL-12, GM-CSF, cytokine

15. NUMBER OF PAGES
31

16. PRICE CODE

17. SECURITY CLASSIFICATION OF REPORT	18. SECURITY CLASSIFICATION OF THIS PAGE	19. SECURITY CLASSIFICATION OF ABSTRACT	20. LIMITATION OF ABSTRACT
Unclassified	Unclassified	Unclassified	Unlimited

Table of Contents

Introduction

Carbohydrates are the most abundantly expressed self-antigens on tumor cells and consequently they are perceived as viable targets for immunotherapy. Aberrant glycosylation of membrane components due to specific alterations of glycosyltransferase activity is a common feature of carcinoma cells and is usually associated with invasion and metastasis. Examples of tumor-associated carbohydrate antigens include GD2, GD3, fucosyl GM1, Globo H, STn and the neolactoseries antigens sialyl-Lewis x (sLex), sialyl-Lewis a (sLea) and Lewis Y (LeY). While pure carbohydrate antigens elicit diminished immune responses because of their T cell independent nature, conjugate vaccine technology has overcome some of these limitations of carbohydrates as vaccines because of the T-dependent (TD) help conferred by the carrier protein. However conjugation of carbohydrates to a carrier protein that elicit carrier-specific T and B cell responses does not necessarily enhance carbohydrate immunogenicity. Furthermore, as there are many carbohydrate types expressed on a tumor cell it may be impractical to develop multivalent vaccines that target each of the surface expressed carbohydrate antigens. Consequently, new formulations or alternative ways to augment carbohydrate immune responses are being evaluated. One alternative that we are pursuing is the development of peptide mimics of core carbohydrate structures expressed on the tumor cell surface. These core structures would be reflective of conformational similarities among what are other wise considered dissimilar carbohydrate antigens. The identification of such peptides would simplify vaccine development in that it may reduce the complexity of multivalent vaccines. Such peptides would function as surrogates of broad-spectrum antigens.

Our studies have evolved to focus on two aspects. One, to better define carbohydrate targets on breast cancer cells that are important in defining their tumor phenotypes and two to develop new formulations or alternative ways to augment carbohydrate reactive immune responses. During the current funding period we have 1.) further examined the murine 4T1 model as a prototype breast cancer cell line defining tumor cell characteristics associated with E and P selectin binding; and 2.) showed that immunization with peptide and DNA form of a rationally chosen peptide mimic, using a lectin reactive profile with 4T1 cells as a template to define carbohydrate types, induces a significant increase in survival rate of tumor-bearing animals in this murine mammary tumor model which is mediated by apoptosis. In the previous year we demonstrated that a peptide mimicking breast associated carbohydrate antigens are capable of activating a carbohydrate specific cellular immune response [Monzavi-Karbassi, 2004 #9] that limits tumor growth in vivo. Thus, carbohydrate-mimicking peptides represent a new and very promising tool to augment immune responses to tumor associated carbohydrate antigens.

Task 1. Establish murine breast tumor model (months 1-3). The purpose of this task was to develop a model cell line expressing carbohydrate antigens relevant to breast cancer. We chose the 4T1 tumor model based on its tumorgencity, high metastatic potential and similar characteristics with human breast tumors in that 4T1 can metastasize to the lung, brain, liver and bone. However, using monoclonal antibodies FH-6 reactive with dimeric sLe^x, BR-55 (LeY specific), CA19.9 (sLe^a specific) and Cslex (sLe^x specific) in FACS, we established that 4T1 cells do not express epitopes reactive with these antibodies. In order to use 4T1 cells as a relevant breast model for evaluating our

mimotopes, we planed to transfect the 4T1 cell line with fucosyltranferases required to generate constituents of neolactoseries antigens in order to express these antigens on the cell surface. During the course of our studies we did come to realize that the 4T1 cell line did expressed a sLe^x epitope reactive with the monoclonal antibody KM93.

The expression of sLe^x and sLe^a by epithelial carcinomas is thought to facilitate metastasis by promoting adhesion of the tumor cells to selectins on vascular endothelial cells. However, experiments supporting this concept by-pass the early steps of the metastatic process employing tumor cells that are injected directly into the blood. While we were developing our model we investigated the relative role of sLe^x oligosaccharides in dissemination of breast carcinoma, employing the 4T1 spontaneous metastasis model (manuscript #1 submitted). The relative mechanistic roles of selectin ligands in mediating tumor cell dissemination and organ colonization have relied on assessing cells that have been transfected or transduced with genes that affect the expression of E-and P-selectin ligands in experimental metastases models in which tumor cells are injected directly into the blood stream. But selectin ligands might impact earlier steps of the metastatic cascade. It would be advantageous to use a model in which tumor cells are injected into a primary site and tumor cell dissemination and distant organ colonization is then assessed.

The phenotypic properties of a sLe^x deficient 4T1 mammary tumor-cell subpopulation isolated by negative selection using the sLe^x-reactive KM93 monoclonal antibody was explored. Carbohydrate profiling of the tumor cell surface reveals that cells collected by negative selection exhibit considerably modified levels of sialylation and fucosylation. Cells negatively selected do not express sLex and lose E-selectin binding but retain P-selectin binding. *In vitro* phenotyping of the tumor cells suggests that both KM93-Neg and Pos cells grow at the same rate; however, KM-93Neg cells are able to detach from the primary site and migrate more efficiently to the distant metastatic sites. All mice inoculated in the mammary fat pad with both negatively- and positively-selected 4T1 cell variants produced lung metastases. However, the number of clonogenic lung metastases is significantly increased in the group inoculated with the sLex negative variant ($P = 0.0031$) indicating that sLe^x functionally decreased metastatic potential of breast cancer cells in this model. This suggests that the inhibition of tumor cell escape from the primary tumor by sLe^x expression may have a greater overall effect on metastatic efficiency than promotion of extravasation through adhesion at distal sites.

Producing cell variants

First, we examined the binding profile of several monoclonal antibodies against cell surface Lewis antigen-related epitopes known to be important in the metastasis process. Among monoclonal antibodies tested, only KM93 which is directed against sLe^x reacts with 4T1 cells as assessed by FACS (Table 1 & Fig. 1A). Notably, sLe^a reactive NS19-9, monoclonal does not react with 4T1 cells (Table 1 & Fig. 1A). This observation is consistent with early studies that indicate that sLe^a serves as a ligand associated with cancer cells derived from the lower digestive organs, while the sLe^x determinant is found to predominate in the adhesion of breast, ovarian and pulmonary cancer cells. The KM93 antibody, reacts with sLe^x antigen with broad specificity and binding assays indicate that this antigen is abundantly expressed on the surface of 4T1 cells.

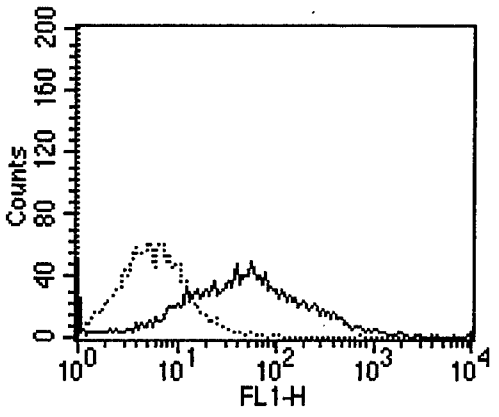

Figure 1A. Km93 binds to parental 4T1 cells. Dotted line is murine IgM (10 ug/ml), which was used as negative control. Continuous line shows KM93 (10 ug/ml) reactivity. Anti-mouse IgM-FITC was used as secondary antibody.

Table1: Mean Fluorescence Intensities of lectins and monoclonal antibodies reactivity with cell populations by flow cytometry.

Lectin/MAbs	Cell variant		
	4T1	KM93-Neg	Km93-Pos
ABL	5.2(±2.4)*	5.7(±2.09)	5.6(±2.3)
ACA	8.8(±1.11)	8(±1.78)	7(±1.41)
SNA	23.28(±5.45)	17.93(±2.8)	16.82(±2.22)
ECL	29.33(±2.36)	15.84(±1.76)	25.3(±2.49)
GS-I	28.6(±4)	30.6(±2.81)	33(3.17)
PNA	10.4(±1.76)	9.9(±0.9)	10.71(±1.5)
VVL	10.21(±1.29)	11.37(±2.18)	11.36(±0.76)
SWGA	nd	42(±2.98)	39.2(±2.87)
BRA-4F1	6.5(±1)	5.78(±1)	5.26(±1)
FH6	6.47(±1)	5.38(±1)	5.63(±0.8)
CA19-9	5.52(±1)	6.74(±0.5)	5.76(±1.18)

- Average of mean fluorescence intensities ± SD based on three replications is shown
- nd, not determined

To study the role of the sLe^x antigens in the metastasis of the 4T1 cell line, cells were sorted based on two criteria (high binding and low binding) determined *via* KM93 reactivity, and two segregated subpopulations were consequently produced. These subpopulations were designated as KM93-Pos and KM93-Neg. Following isolation, we tested reactivity of KM93 antibody with the cell variants produced (Fig. 1B). Experimental results show a non-overlapping peaks in KM93 reactivity between the two subpopulations in FACS analysis.

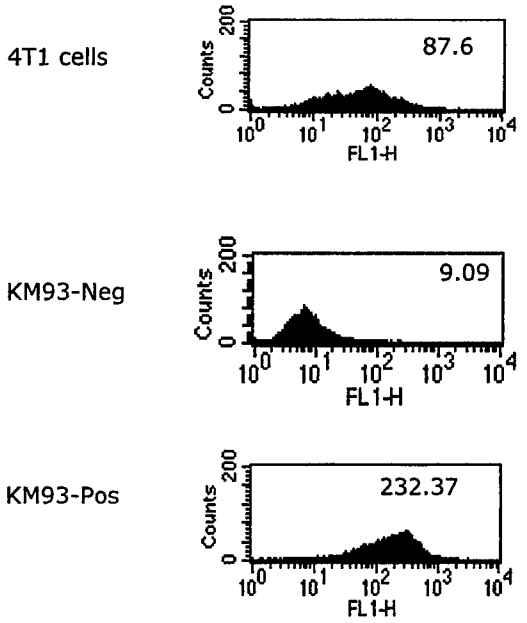

Figure 1B. Km93 staining of produced variants. 4T1 cells were sorted three times for induction of negative and highly positive KM93-reactive subpopulations. Expression of sLex epitope was tested in original 4T1 as well as in KM93-Neg and KM93-Pos subpopulations.

Characterization of cell surface carbohydrates.

Cell sorting could lead to enrichment of minor subpopulations that differ in other cell-surface oligosaccharide structures. The cell surface glycosylation patterns of the subpopulations were determined. We used monoclonal antibodies and a panel of plant lectins to characterize alterations in carbohydrate structures on the cell membrane as illustrated in Table 1 and Figure 2. ABL (*Agaricus bisporus,* mushroom, lectin) and ACA (*Amaranthus caudatus,* lectin) do not react with either the KM93-Pos or KM93-Neg variants indicating that there is no expression of Thomsen-Friedenreich (TF) antigen, Galβ(1→3)GalNAcα, or sialylated TF on the cell surface. Consistently, the TF-specific lectin PNA (*Arachis hypogaea,* peanut, agglutinin) also did not react with either cell subpopulation. VVA (*Visia villosa,* hairy vetch, agglutinin), which has specificity towards the Tn antigen (GalNAc-α-R), does not distinguish between the cell variants, indicating similar levels of Tn antigen expression. Both GS-I (*Griffonia simplicifolia*) and SNA (*Sambucus nigra,* agglutinin), which are specific for the α-Gal epitope and α(2→6) sialic acid, respectively, react identically with both subpopulations. ECL (*Erythrina critagali,* lectin) shows a slight increase in reactivity with the KM93-Pos variant and is specific for Galβ(1→4)GlcNAc, suggesting that positive selection for the KM93 epitope exposed more type II chain LacNAc, a major component of most N-linked structures including sLe^x.

As shown in Figure 2, WGA (*Wheat germ agglutinin*), which is specific for both GlcNAc and sialic acid, shows a significant increase in binding to the KM93-Pos cells suggesting elevated levels of either one or both of these structures. To distinguish between GlcNAc and sialic acid, we tested the binding of succinalated WGA (Table 1), which binds to only GlcNAc residues and not sialic acid. Succinylated WGA did not differentiate significantly between the two subpopulations, implying that the higher WGA binding to the positive variant is most likely due to an increased level of terminal sialic acid. The decrease in sialic acid on the surface of the KM93-Neg variant is most

likely that of the α(2→3) linkage type (comparison of SNA binding vs. WGA binding between the two variants). *Ulex europaeus* (UEA-I) lectin, which reacts mostly with terminal α(1→2) linked fucose residues [35], was also tested for binding (Fig. 2) and displayed significantly higher reactivity with the KM93-Pos variant. Taken together, the lectin binding profile suggests that negative selection for the KM-93 reactive epitope has resulted in a decrease in sialic acid and of terminal α(1→2) mono-fucosylated structures. Monoclonal antibodies to Lewis x (Lex, BRA-4F1), sialylated dimeric Lewis x (FH6) and sLea (NS19-9) did not show reactivity with 4T1 cells or its variants (Table 1). Based on data obtained from GS-I binding, we believe that chain termination in the KM93-negative population has not been replaced with either sialic acid or αGal. Since UEA is specific for a(1-2) monofucosylated structures but not further modified by glysosylation such as difucosylated LeY structure or blood group A and B structures we can not conclusively conclude whether a1,2 fucosyltransferase is responsible for decreased expression of SA-Lex.

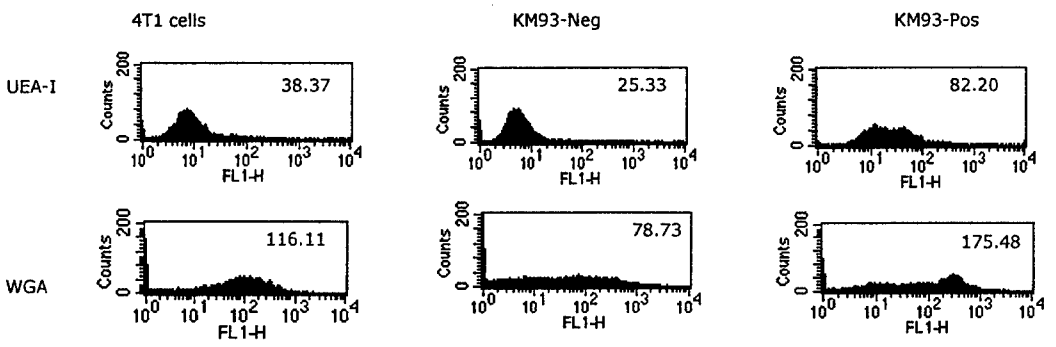

Figure 2. WGA and UAE-1 lectins react differently to the cell variants. Mean fluorescence intensity for each histogram is shown.

To corroborate the above observation, NMR spectroscopy was employed to further characterize cell surface glycan structures. ^{1}H NMR spectra of intact cells confirmed a decrease in cell surface sialic acid (1.91 ppm) in KM93-Neg cells, corroborating the WGA lectin binding data (Figure 3A). In KM93-Pos cells, the fucose resonance at 1.2-1.3 ppm is more clearly observable than that in the KM93-Neg (Figure 3B). In addition to the compounds mentioned, a spectral pattern comprised of major resonances at 0.63 ppm, 1.75 ppm, and 2.9 ppm all showing connectivities to one another (verified by COSY spectra [36] is also observable on the surface of KM93-Neg cells yet is either diminished or completely absent from the surface of KM93-Pos cells (Figure 3). Together these results indicate that the KM93 positive and negative variants have distinct cell surface glycosylation patterns. The loss in KM93 reactivity toward sLe^{x} may result from a loss of sialic acid residues from the KM93 reactive carbohydrate epitope.

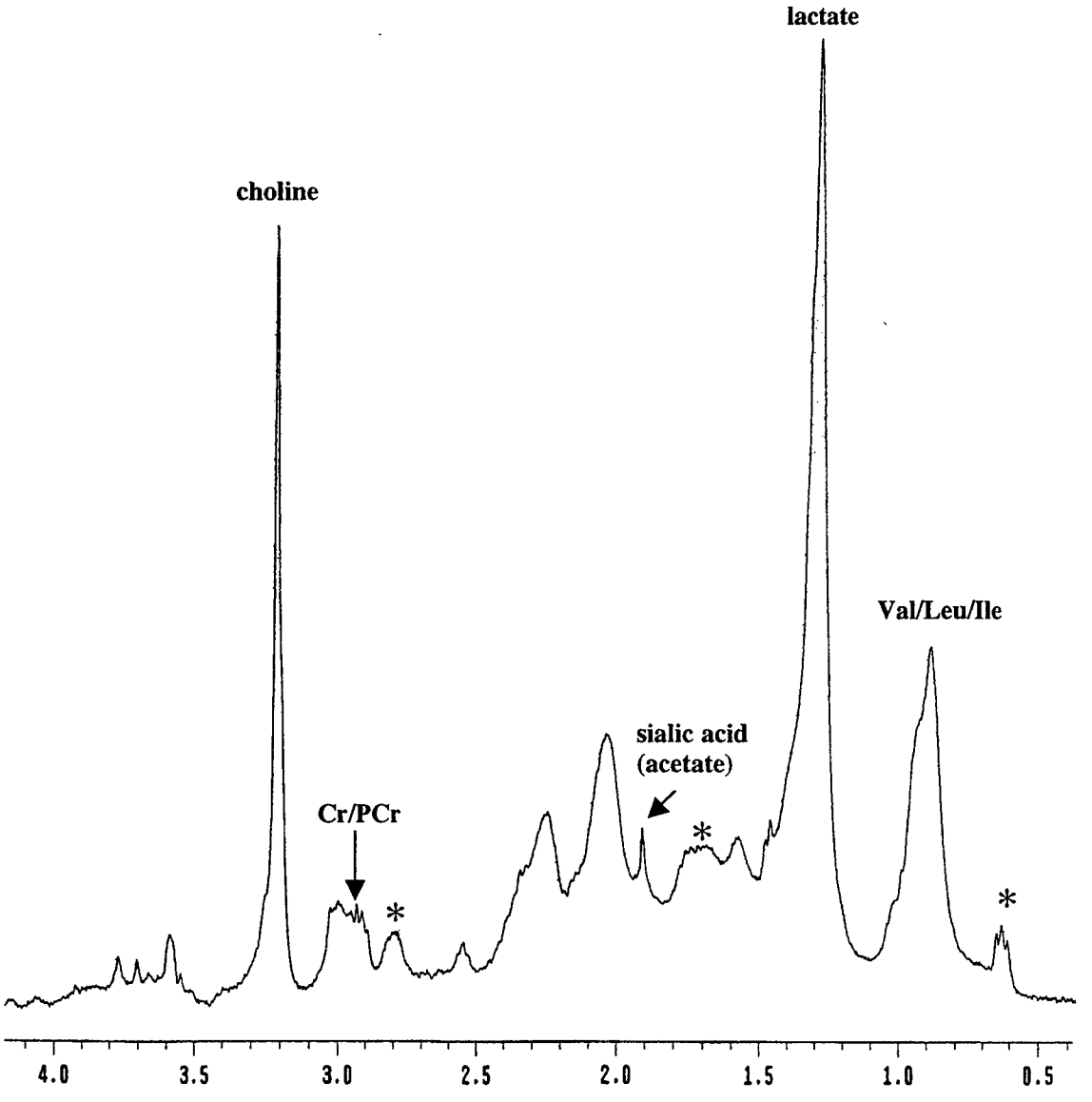
lactate
choline
Val/Leu/Ile
sialic acid
(acetate)
Cr/PCr
*
*
*
4.0
3.5
3.0
2.5
2.0
1.5
1.0
0.5

Figure 3A

Figure 3 B

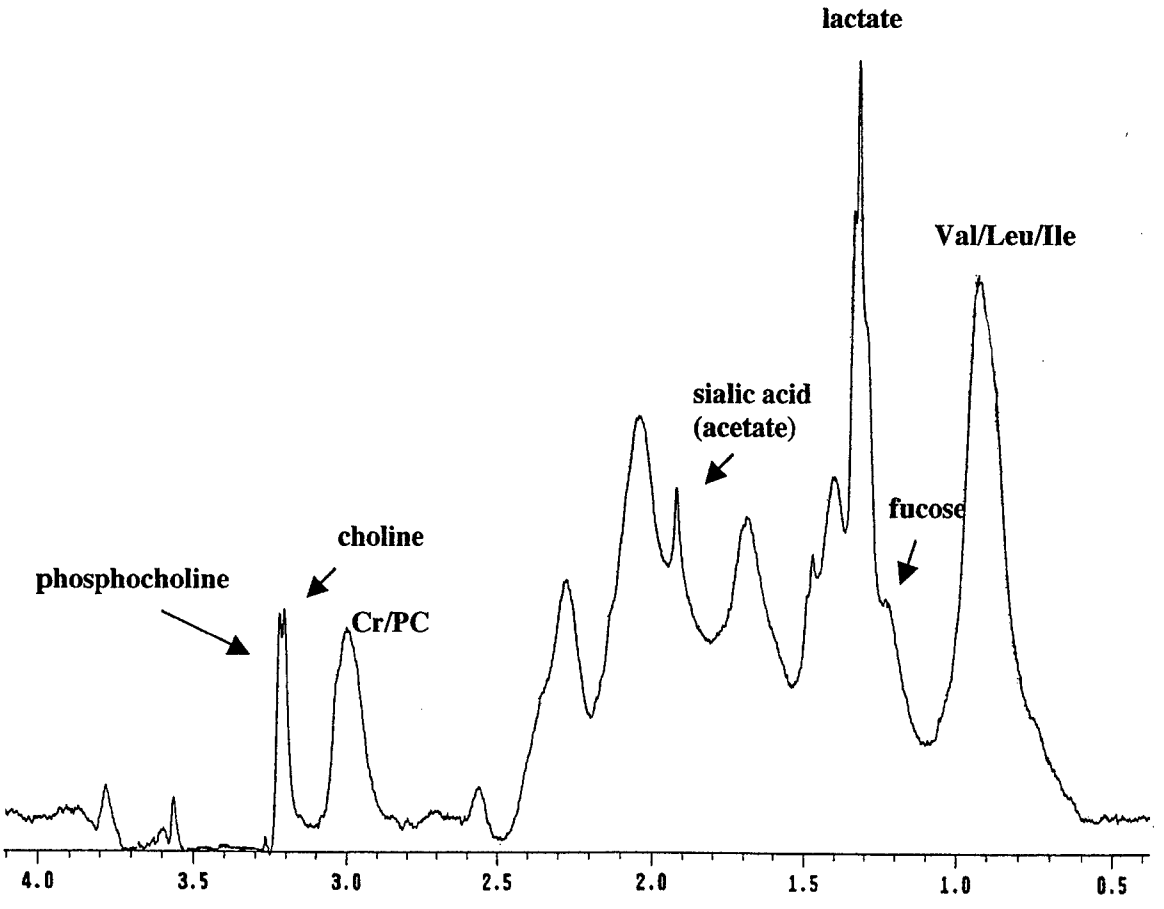

Figure 3. 400 MHz ^{1}H NMR spectra of 10^8 KM93-Neg (A) and KM93-Pos (B) cells. The resonance corresponding to the acetyl group of sialic acid in KM93-Pos is greater than that in KM93-Neg. The fucose resonance is clearly seen in KM93-Pos (absent in KM93-Neg cells), indicating an altered surface fucosylation state. Resonance marked with (*) indicate a triad of resonances that are covalently linked and present only on the surface of KM93-Neg cells.

Reactivity of cell variants with E- and P-selectin chimeric proteins

Murine 4T1 is a highly metastatic cell line, and based on its reactivity with KM-93 mAb, the expression of E- or P-selectin ligand(s) on its surface is expected. To investigate the functional significance of the different cell surface carbohydrate expression patterns, the cells were tested for binding to E- and P-selectin. To determine whether P- and E-selectin molecules react differently with the cell variants, cells were incubated with recombinant mouse E- and P-selectin/Fc (human IgG) chimeras and binding was assayed by flow cytometry. As shown in Figure 4, E-selectin bound weakly to the original 4T1 cells and it's binding increased after positive selection for KM93 reactive epitope. E-selectin did not bind to the KM93-Neg variant. Reactivity of P-

selectin with selected variants remains similar to the levels detected in binding to the parental 4T1 cells. These results indicate that binding of E-selectin to the 4T1 cells correlate with the expression level of its ligand sLe^x. These results further indicate that negative selection resulted in a cell line deficient in the biosynthesis of E-selectin ligands that may include sLe^x as other cell variants lacking sLe^x expression still retain E-selectin binding.

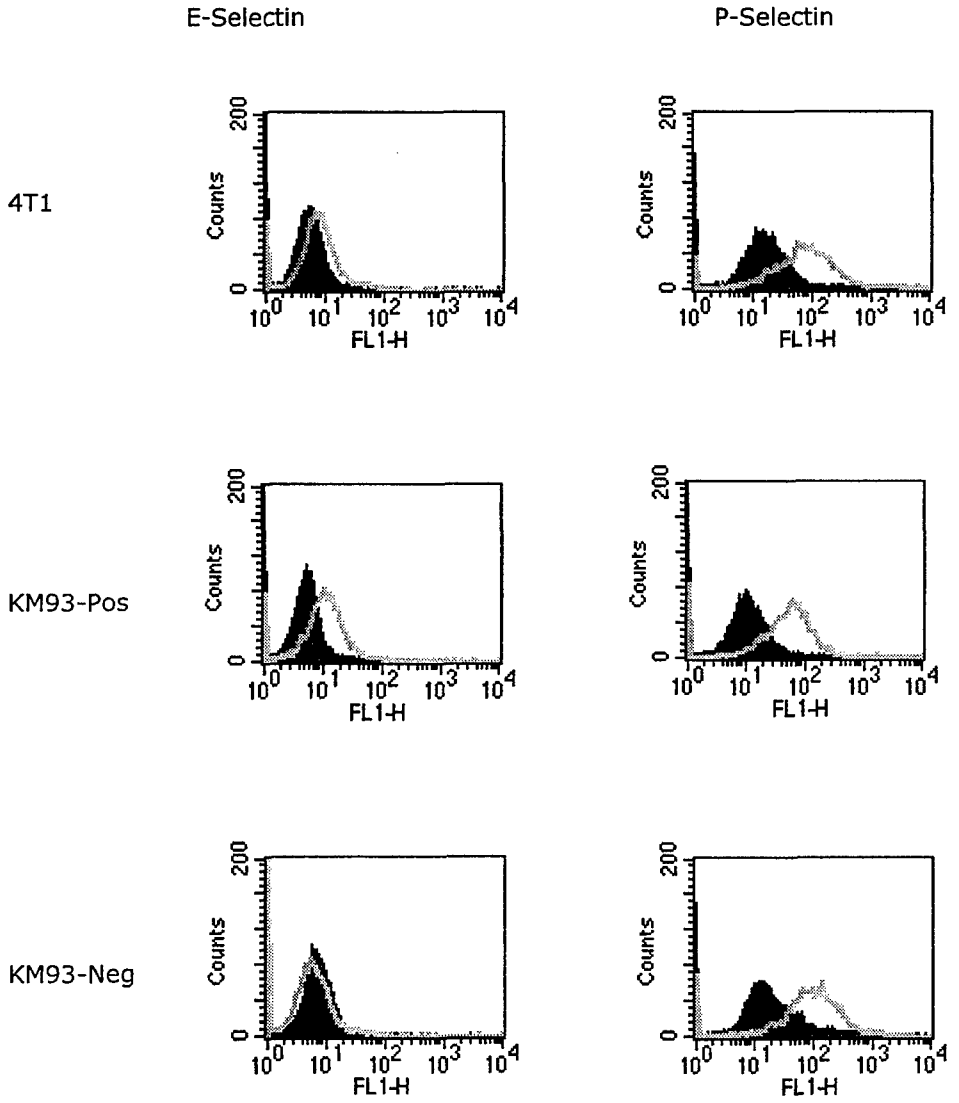

Figure 4. Flow cytometric analysis of mouse E- and P-selectin binding to the 4T1 cells and its KM93-Neg and –Pos variants. Cells were first incubated with IgG-chimeric proteins and then stained with FITC-conjugated goat anti human IgG (open histograms). Filled histogram is the binding in the presence of 20mM EDTA.

Tumor cell adhesion to HUVEC cells.

To further clarify the binding properties of the cell variants, monolayer of HUVECs were prepared and adhesion of the parental 4T1 and other selected cell variants to them was determined (Fig. 5). Binding of parental 4T1 cells and its variants to HUVECs was increased between 60 to 100% after TNF-α treatment, however, no significant differences in adhesion after treatment with TNF-α among the cell types was observed (data not shown). TNF-α treatment has increased the expression of E-seletin more than 100 times as assayed by flow cytometry (data not shown). Data imply that binding to endothelial cells might not be affected by either the positive or negative selections for the KM93 epitope.

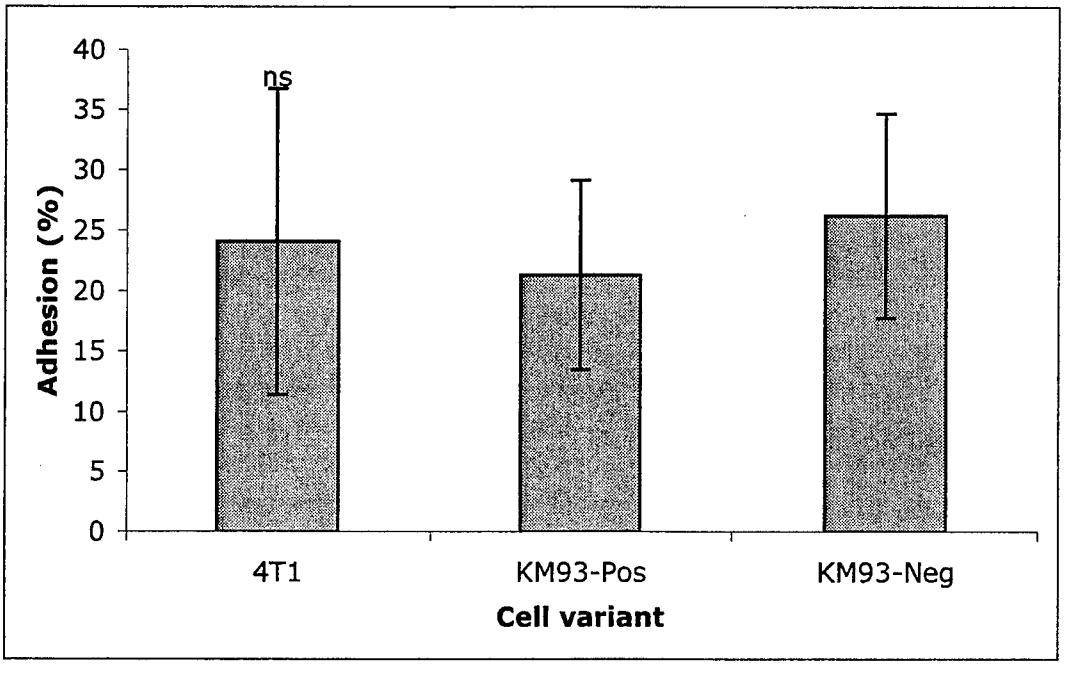

Figure 5. Adhesion assay of tumor cells to HUVECs. Monolayer of HUVECs was prepared and activated with TNF-α, cell variants were labeled with calcein AM and co-incubated with HUVECs for 60 min. Then unbound cells were washed out, fluorescence measured and percentage of adhesion was calculated. Bars are standard deviation of means of four independently performed assays. ns, no significant differences between cell variants were detected.

Invasive ability and apoptosis sensitivity of tumor cells

To further explore and compare relevant characteristics among cell variants, we performed Matrigel™ -based invasion assay and an apoptosis related assay to see if the selection has changed sensitivity of cells to apoptosis or their invasive ability. We did not observe significant differences between cell variants regarding their ability to invade Matrigel™ or their sensitivity to starvation-induced apoptosis (data not shown).

***In vitro* growth characteristics of cell variants**

Comparison of cell growth *in vitro* revealed a similar growth rate for both KM93-Neg and -Pos subpopulations (Fig. 6A); however, the growth pattern is different (Figure 6B). The KM93-Pos variant, which is similar to the original 4T1, tends to grow in clusters with high densities. While clusters are also visible in the KM93-Neg variant, this cell type has a tendency to spread out individually and quickly on the plate surface. Shortly after seeding the cells *in vitro*, KM93-Neg cells was observed to scatter, covering the surface, while KM93-Pos cells grew in separated clusters with surface void volume in between. To evaluate the rate of migration, we conducted a wound healing experiment (Fig. 6C). As illustrated, 24 hours after scraping KM93-Neg cells begin to cover the scraped surface on the dish, and at 48 hours later the progress is obvious. In the same time frame, KM93-Pos cells have yet to form separate colonies on the bare surface. These results suggest that selection for the carbohydrate epitope significantly changed the in vitro adhesion properties of the cells.

Figure 6A)

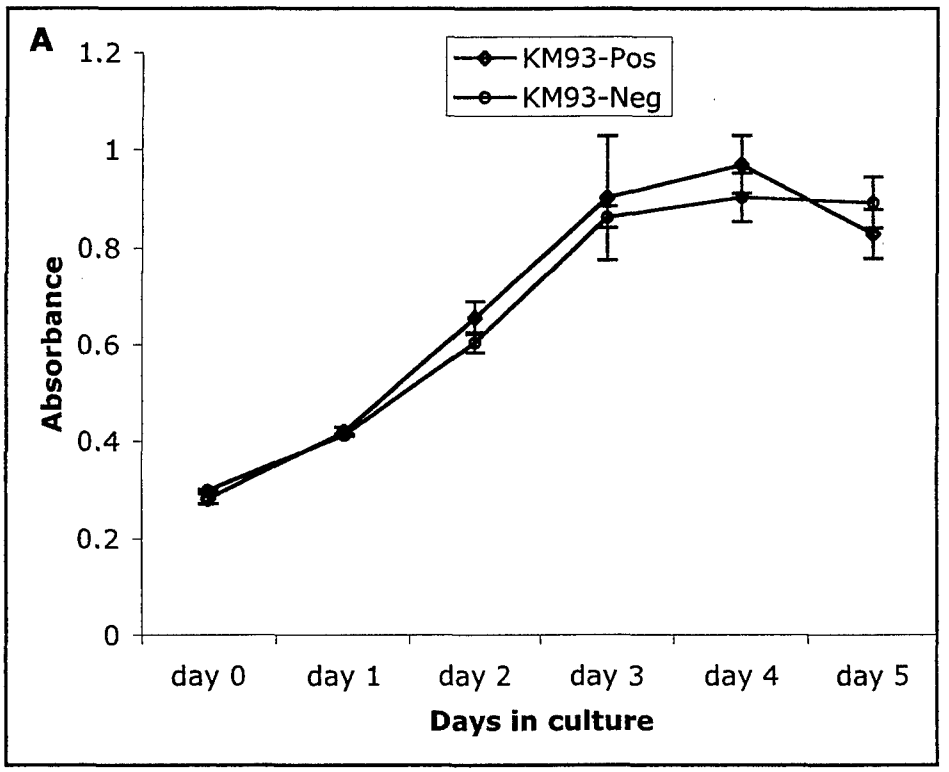

Figure 6B)

KM93-Neg

KM93-Pos

Day 2

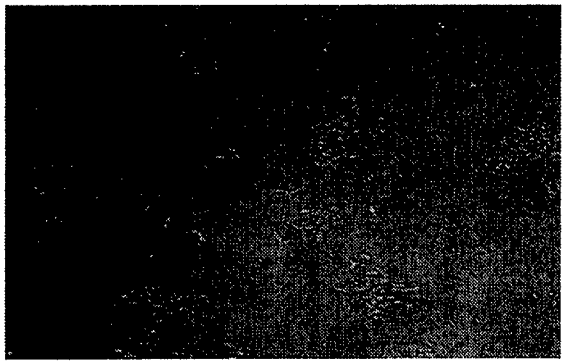

Day 3

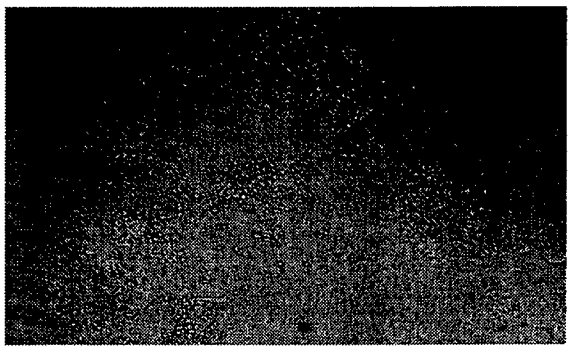

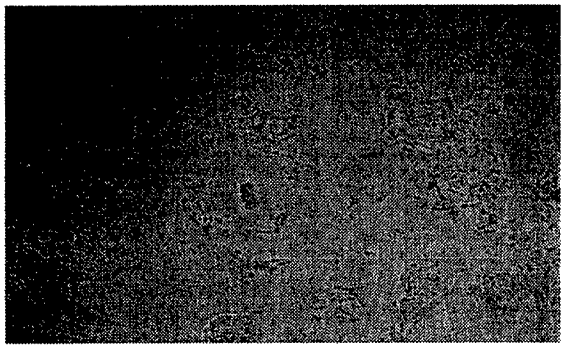

Day 4

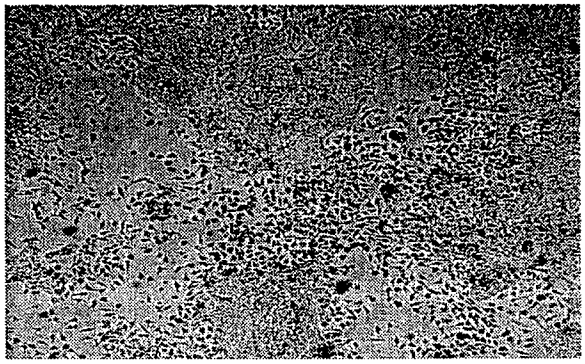

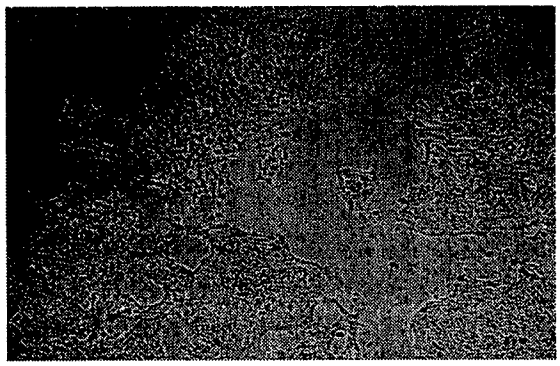

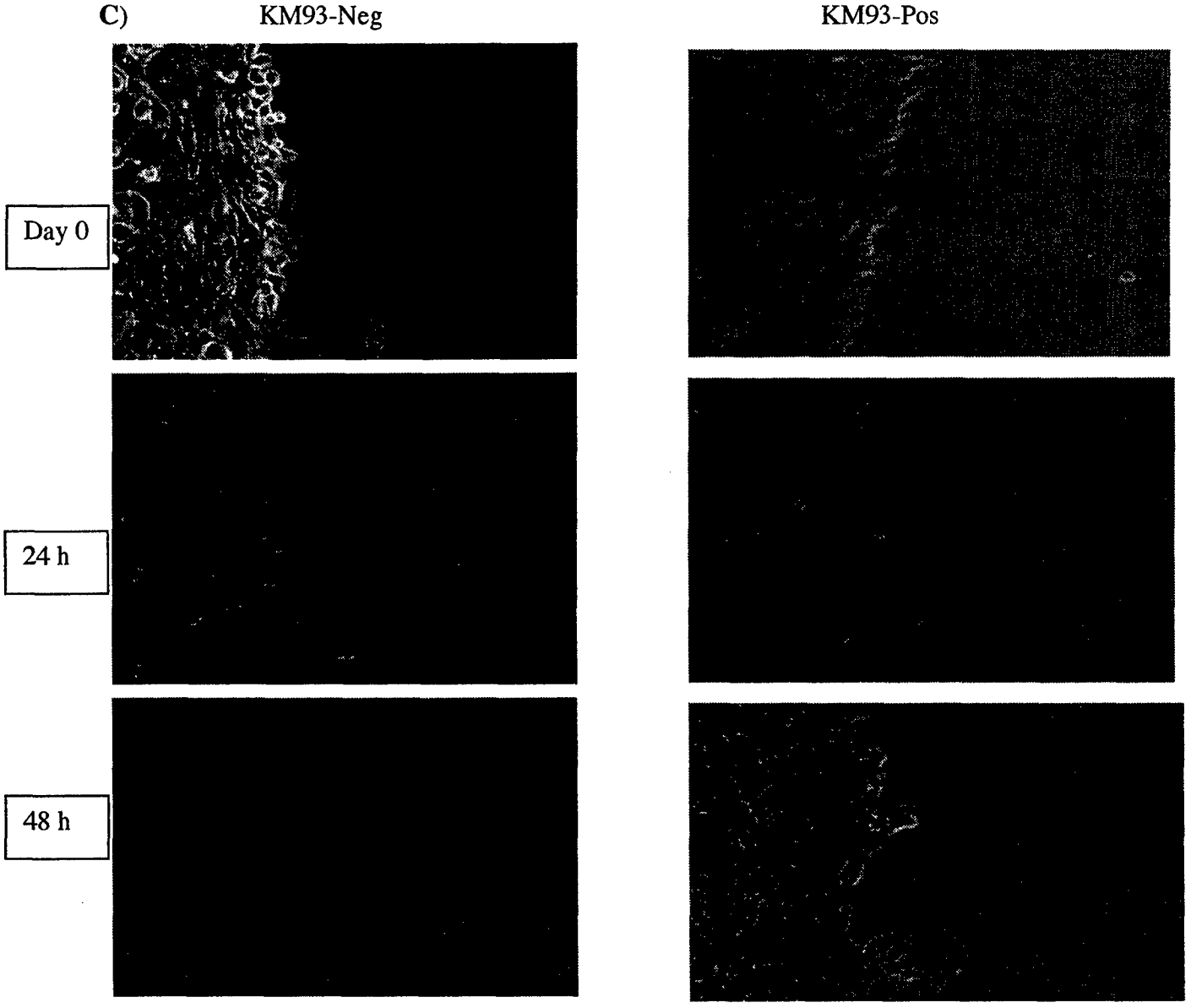

Figure 6. Phenotype of KM93-Neg and KM93-Pos *in vitro*. A) The same number of cells (5000/welll) was seeded in wells of a 96-well plate at the day zero and cell proliferation was assessed using MTS assay as described in materials and methods. Bars show SD of three replications. **B)** Wells were photographed on days 2, 3 and 4 and representative images are shown. **C)** The same number of cells was seeded into 100mm tissue culture plates and when the cells were grown to confluent state, the cell layer was scraped in the middle of the plate. Photographs were taken at the time of scraping, 24 hours and 48 hours later as indicated.

Tumor growth and metastasis *in vivo*.

sLex on the surface of tumor cells is thought to promote metastasis by enhancing adhesion of tumor cells to endothelia in the vascular beds of distal organs. This in turn is thought to facilitate extravasation of the tumor cells and promote establishment of metastases. Much of the evidence supporting the role of sLex in the late stages of metastasis is derived from experimental animal models where the tumor cells are introduced directly into the peripheral blood. In these models, the tumor cells by pass all of the early barriers to metastasis that tumor cells arising in the breast or other tissues of origin must successfully negotiate [4]. Here we investigated possible differences in spontaneous metastasis using a mouse model that requires tumor cells to go through all steps of the metastatic process. Tumor transplantation with the cell variants was performed to evaluate their metastatic tendency. Groups of mice were inoculated with both the positively- and negatively-selected subpopulations to compare tumor growth and metastasis (Fig. 7). We observed a statistically significant ($P = 0.0031$) higher number of established metastatic cells in the lung for KM93-Neg cells (Fig. 7A).

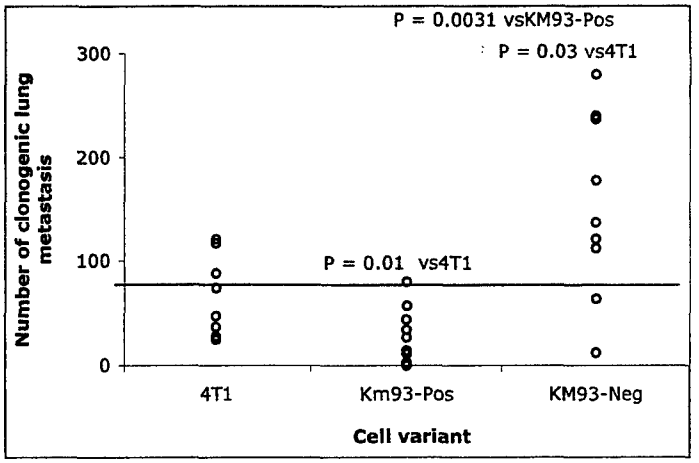

Figure 7A. Km93Neg metastasize more to lung than Km93Pos and original 4T1 cells. Mice were inoculated into the mammary fat, sacrificed at day 26, organs removed, cell suspensions prepared and cultured. Number of clonogenic lesions was plotted. The continuous line shows the overall average of all individual tested in the experiment

When compared to the original 4T1 cell line, the number of cell colonies observed by clonogenic assay in mice inoculated with both the KM93-Pos and –Neg variants was significantly different in the same incubation time period. The growth of primary solid tumor evaluated by the tumor size was not different among the selected cell variants in early stages. As shown in Figure 7B, we compared KM93-Neg and –Pos and observed a statistically significant larger tumor size in KM93-Neg inoculated mice near the end of the experiment (at days 21 and 26 post-transplant). Comparing the tumor size in parental 4T1 with either cell variant in all dates, we did not detect significant differences (data not shown). We do not know the exact reason for the late segregation in tumor size observed between KM93-Neg and -Pos cells, it might be a micro-environmental effect or simply due to the strong homotypic adhesiveness among Km93-Pos cells. We ran a correlation test between the size of tumor at the time of harvest and the number of the clonogenic cells and observed a small, statistically not significant correlation coefficient (r=0.46) in KM93-Neg population. The calculated r indicates that only 20% of variation in the

number of metastatic tumor cells in lung could depend on the size of tumor measured, which is not meaningful.

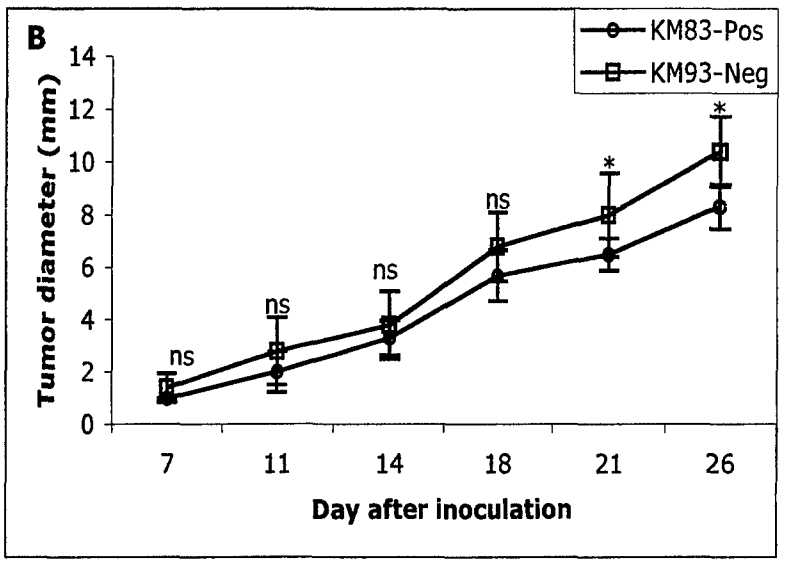

Figure 7B. Km93Neg metastasize more to lung than Km93Pos and original 4T1 cells. Average of tumor diameter for mice in each group over the period of time after inoculation up to sacrifice is shown. * significant at $P < 0.05$ as performed by Students t test. The experiments were repeated three times.

Task 2. To evaluate immune parameters associated with DNA vaccination of plasmids encoding glycotope (months 1-16).

Metastatic disease, mainly to the lungs, liver, bone, and brain, is the most common cause of death from breast cancer. Induction of a systemic immune response to common tumor-associated antigens (TAA) is proposed as a general approach to eradicate metastatic lesions. Tumor cells, however, escape an ongoing immune response using various mechanisms including loss of target antigen and down regulation of MHC molecules or disruption of complement cascade. Therefore, employing novel anti-tumor immunological mechanisms in the immunotherapy array are needed. Apoptosis is a natural anti-tumor weaponry used by the organism to arrest growth of transformed cells. Natural carbohydrate reactive IgM antibodies are implicated in mediating apoptosis of tumor cells and these circulating natural antibodies are suggested as a mechanism of innate immune surveillance against cancer cells. The selective targeting of tumor associated carbohydrate antigens by induction of serum antibodies that trigger apoptosis as a means to eradicate tumor cells would therefore be an advantage in vaccine development (manuscript #2 submitted).

Choice of peptide mimotope

Arrays of peptide mimotopes have been developed in our Laboratory over the years. We screened several of them for binding to the lectin GS-1 that is reactive with the murine Gal epitope and with the human antigens Leb and LeY. Peptide mimotopes shown in Table 2 were screened for reactivity against GS-1. We observed that GS-1 binds predominately to peptides 107 and 105 (manuscript # 2 submitted). We observed that only peptide 107 bound to GS-1 in a dose-dependent manner. In an inhibition assay, the peptide 107 significantly inhibited GS-1 lectin binding to the cells.

Table 2. Peptides used in the study

Peptide	Sequence
104	GGIMILLIFSLLWFGGA
105	GGIYYPYDIYYPYDIYYPYD
106	GGIYWRYDIYWRYDIYWRYD
107	GGIYYRYDIYYRYDIYYRYD
109	GGARVSFWRYSSFAPTY

The 107 peptide was chosen for our studies based on its consistent reactivity with GS-1 (manuscript #2 submitted). Previous studies have indicated that immunization with this peptide produce serum antibodies able to mediate complement dependent cytotoxicity on Meth A and MCF7 cells, which inhibited Meth A cell growth in vivo.

DNA Immunization results in induction of serum antibodies reactive with 4T1 cells
We have previously shown that immunization with peptide mimotopes of carbohydrate antigens formulated as multiple antigen peptides or as DNA vaccines can elicit carbohydrate reactive IgM serum antibodies. To expand this later strategy, the sequence of peptide 107 was translated into oligonucleotides and DNA constructs were developed in a secretory (pSec) plasmid from Invitrogen (Manuscript # 2 submitted). Groups of mice were immunized with the 107-peptide-encoding DNA constructs and serum reactivity with 4T1 cells was detected by FACS (Fig. 8). We detected anti-4T1-cells serum antibodies of IgM isotype, with no cell-specific IgG isotype detected. Serum antibodies mediated cell death upon Co-incubation with 4T1 cells. In order to assess serum-mediated cell cytotoxicity, cells were co-incubated with serum from peptide encoded DNA- or vector-alone immunized mice and the percentage of dead cells was detected after overnight co-incubation. We observed 20% dead cells in wells containing 107-pSec serum in comparison with wells supplemented with vector-immunized serum. In concert with the GS-I effect, immunization-generated serum mediated apoptosis of 4T1 cells (Fig. 9).

Figure 9. Serum response to DNA immunization. Mice (10/group) were immunized three times with 107-coding sequence and the respective vector plasmid pSec. Animals were bled 10 days after the last boost. For each group sera were pooled for 10 mice. Binding of serum antibodies to 4T1 cells was detected by FACS and presented by mean fluorescence intensity (MFI).

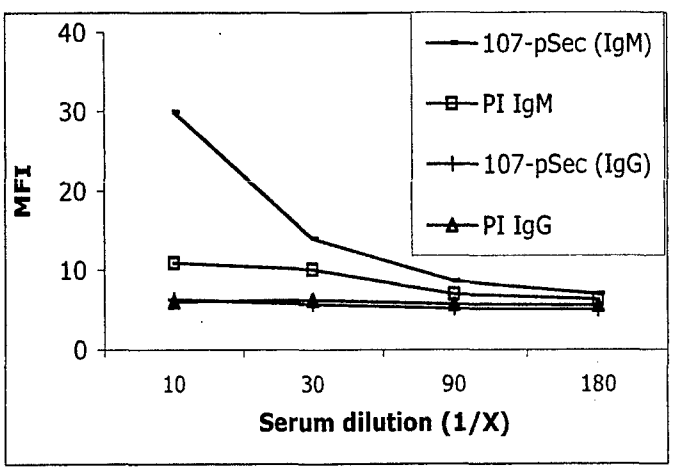

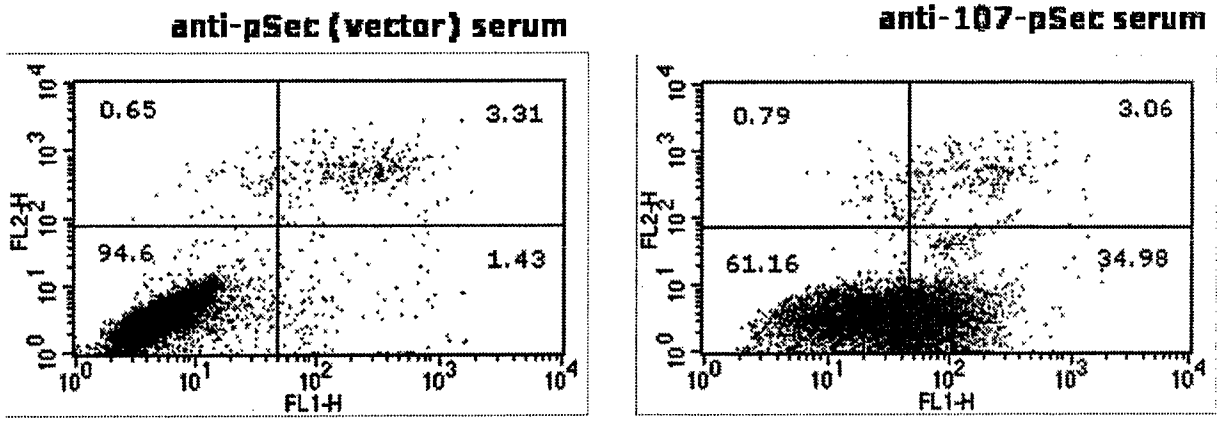

Figure 9. Serum mediates apoptosis in 4T1 cells. 4T1 cell were incubated for 16 hours with serum from 107-pSec and pSec only immunized mice. DMEM medium was supplemented with 10% of murine serum as indicated. Then cells were harvested, washed, stained with propidium iodide (FL-2) and annexin V(FL-1) and analyzed by FACS.

DNA immnization was next compared with peptide immunization. Mice were bled 7 days after the third immunization. Serum was collected individually and all sera were pooled for 10 mice in each group. Binding of pooled serum to 4T1 cells and its apoptotic activity was assayed (Table 3). As shown in the Table 3 immunization with both peptide and DNA formulated vaccines generates serum antibodies that bind to 4T1 cells and mediate apoptosis of this cell line. The Peptide formulated vaccine immunization generates antibodies of higher end point titer, which mediated a more pronounced apoptotic effects.

Table 3. Characterization of serum after DNA and peptide immunization.

Test description	Peptide immunization			DNA immunization			GSI
	Naive	106	107	PSec-vector	PSec-106	PSec-107	
Endpoint titer[+]	_	1:1280	1:2560	_	1:160	1:160	_
Annexin binding[++]	184 (±39)	228 (±53)	436 (±64)	171.5 (±43)	244.5 (±32)	324 (±36)	902
PI binding[++]	32	29.8	32	40.33	38.58	52.29	111

[+]Binding of IgM antibodies to 4T1 cells was tittered. Titer was determined based on mean fluorescence intensity (MFI) of flow cytometry assay. The highest serum dilution with higher MFI than the pre-immune serum is shown as the end-point titer.
[++] MFI for annexin V (± standard deviations) and propidium iodide (PI) is shown.

Caspase activity

To further explore and compare pathways involved governing observed apoptotic effects, we examined activation of caspase 2, 3, 8 and 9 in 4T1 cells after treatment with the lectin and the serum from peptide 107 immunized mice (Table 4). Overnight incubation with the GS-I lectin induced activation of all caspases tested. Further experiments were performed to identify the first caspase activated. As shown in Table 4, after 4 and 6 hours of co-incubation with the lectin, caspase 3 followed by caspase 2 are the first caspases that could be detected. We also tested activation of the same caspases after co-incubation of cells with the serum overnight. We detected activation of all caspases after over night incubation of cells with serum from 107-immunized mice but not with sera from peptide106-immunized or naïve mice (data not shown). Further, when we compared the level of activation of caspases at 4 and 24 hours of co-incubation with the peptide 107 derived serum (Table 4), we observe that similar to the lectin, Caspase 3 and Caspase 2 act as the major players in mediating apoptosis of 4T1 cell.

Table 4. Caspase activation.

4T1 cells	Caspase			
	II	III	IIX	IX
Control, regular medium	8523(± 5382)	36893 (±16071)	2405 (±856)	1478 (±553)
GSI, 10ug/ml overnight	25809.13 (±12115)	58029 (±4227)	6942 (±3886)	3048 (±1648)
GS1, 10 ug/ml 4 h+	348	12806	286	0
GSI, 10 ug/ml 6 h+	2648	11045	675	125
Peptide 107-immunized serum++	6245.84	20795.36	1001.04	282.33

+ values for the control cells (not treated) are subtracted.
++ cells were incubated for 4 and 24 hours, then the caspase activity was measured. Data shown represent the values after 24 hours incubation subtracted by the values after 4 hours incubation.

Task 3. Evaluate priming and boosting effect of immunogens. (Months 10-20).
We have not progressed further in this area from our last report as we were furthering evaluating our 4T1 responses in Task 4.

Task 4. Perform tumor challenge experiments (months 18-36).
The murine 4T1 breast tumor cell line is a highly metastatic mammary cell line proposed to model metastatic disease in advanced stages metastasizing efficiently to lung, liver, bone and brain after implanting into mammary fat pads and has proven to be weakly

immunogenic and highly aggressive. This animal model closely resembles human breast cancer and is a rigorous model of advanced spontaneous metastatic disease. Clonogenic lesions are first detected in the lung and then liver in a time dependent manner. Lung metastasis is detectable as early as day 14 after transplantation in all mice tested while for liver, this time is around day 28-35 after transplant (Table 5) paralleling observations by others.

Table 5. Incidence of spontaneous metastasis in liver and lung harvested from mice at various times after 4T1 tumor inoculation.

Day post implant	Organs	
	Liver	Lung
20	0/10	10/10
25	1/5	5/5
30	7/10	10/10
33	6/7	7/7

Mice were challenged with 10^4 4T1 cells s.c. in the abdominal mammary gland. Animals were sacrificed at indicated times post transplant, liver and lung harvested and cultured for metastatic cell growth detection. The number of animals positive for metastases of the total number tested each time for each organ is shown.

Therapeutic DNA immunization can arrest liver metastasis

To assess whether vaccination with peptide 107 could arrest metastasis, we established the 4T1 tumor in mammary fat pads and then started immunization with the plasmids containing the DNA sequences of 104, 105 and 107 mimotopes. While immunization with 107-pSec plasmid induced slight tumor shrinkage that was temporary (data not shown) immunization with 107-pSec significantly ($p = 0.021$) increased survival time of the tumor-bearing animals as compared with immunization with vector (pSec) only (manuscript #2 submitted).

To further characterize the effects of immunization on metastasis to distant organs, we repeated the challenge experiment as above and 30 days post tumor transplant, lung and liver samples were harvested and metastatic lesions were quantified (Table 6). The immunization regime had no effect on the lung metastasis but had significant positive effects on reducing liver metastasis (Fisher exact test, $p = 0.018$). Out of 12 mice used for 107 therapeutic DNA immunization only 2 were found positive for tumor in the liver compared with 8 out of 12 positive livers in vector immunized animals.

Table 6. Number of mice detected positive for distant organ metastasis out of 12 total mice.

Immunization	Organs	
	Lung	Liver
pSec (vector)	12	8
pSec-107	12	2*

*$P = 0.018$ as compared with vector immunized by Fisher exact test.

Prophylactic immunization with DNA and the peptide

Therapeutic immunization had no significant effect either on the size of primary tumor or on lung metastasis. This might be because of the late appearance of antibodies in adequate concentration. To test whether or not earlier immunization and accumulation of antibodies at the time of tumor challenge modify the outcome of immunization, in a follow-up study mice were immunized before the challenge and after that with both the peptide and DNA constructs. Mice were bled 7 days after the third prophylactic immunization and then challenged with 4T1 cells 3 days after the blood collect. In both peptide and DNA-immunized animals tumor grew significantly slower. All pre-immunized mice developed tumor upon challenge, however, tumor growth was significantly slower in peptide 107-immunized animals (Fig. 10). We have not observed tumor growth inhibition in our therapeutic immunization regimen. Others have shown that the size of solid primary tumor in this model correlates with the number of established metastatic cells in the lung. We collected lungs at day 28 post tumor transplant from both DNA and peptide immunized mice and performed clonogenic assay. In the peptide-immunized group (with 10 mice per group), 30 percent of 107-peptide immunized animals were detected as free of lung tumor. In addition, comparison of the average of clonogenic lung metastases showed a significant reduction in the 107-immunized group (Fig 10C). In the DNA-immunized group all mice tested had established lung metastasis, however, pSec-107 immunized mice had smaller average of colonies than pSec-106 and pSec vector control (data not shown).

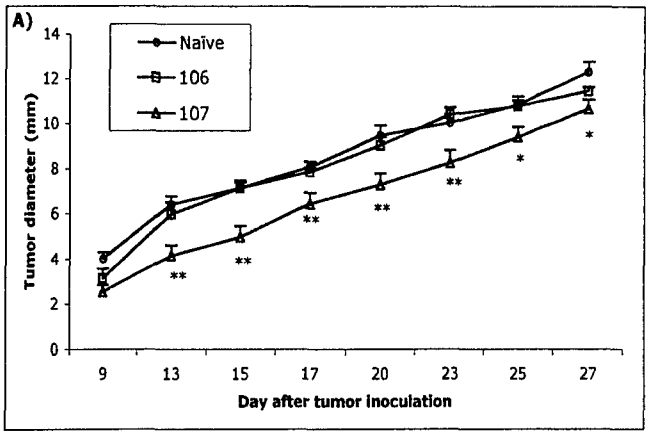

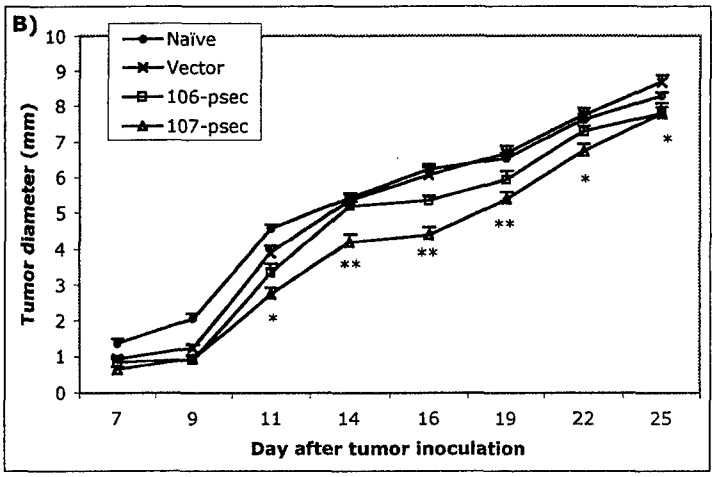

Figure 10. Immunization with the107 peptide inhibits tumor growth and reduces lung metastases. Mice (10 per group) were immunized with peptide (**A**) or DNA constructs (**B**) weekly for three times and then inoculated with tumor at day 10 after the third immunization. Immunization was resumed at day 7 post-transplant and continued for three times weekly. Tumor size was measured during this period of time and are illustrated as the mean values ± SD. *$P < 0.025$; **$P < 0.01$ as compared with 106 (A) or vector (B) immunization.

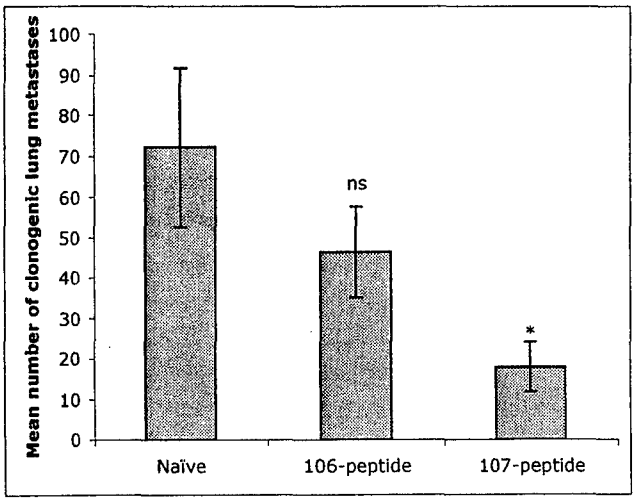

(**C**) Peptide-immunized mice were sacrificed at day 28, lungs were collected and clonogenic assay was performed, number of clonogenic cells was determined and illustrated as the mean values of 10 mice per group ± SD. * $P = 0.009$.

Is the antigen shared with human breast cancer cell lines?

We know that LeY is present on breast tumors. We looked at possible competition between Leb and LeY for binding to the anti-107 serum. ELISA plate was coated with Leb antigen and the anti-serum binding to Leb was abrogated by serial pre-adsorption with both LeY and Leb (Fig. 11). This result implies that the antigen is a common constituent of both antigens meaning that whatever happens in the mouse model might happen in human.

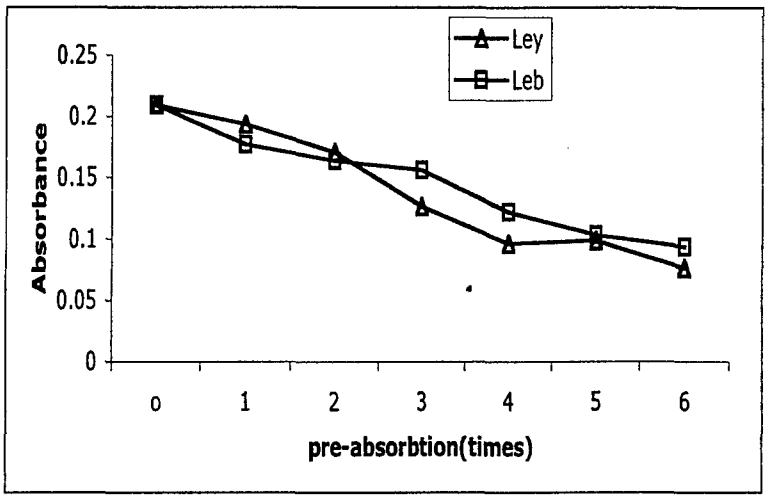

Figure 11. *Mice were immunized with 107 peptide/QS21 and serum was collected. Reactivity of the serum against Leb antigen was detected by ELISA. Reactivity was wipped out by preabsobtion of the serum with both leY and leb antigens.*

We also screened peptides 105, 106, 107 and LeY with human serum from normal patients and Breast cancer patients (n=10). We observed that peptides 106 and 105 were more reactive with serum from Breast Cancer patients over serum from normal patients (controls) out to about 1:800 titer. This distinction was not observed for peptide 107 (data not shown) which maybe explained if we think peptide 107 is a mimic of the Gal epitope in which 1% of total circulating IgG is reactive with.

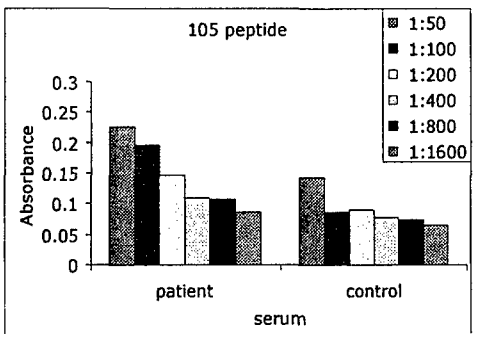

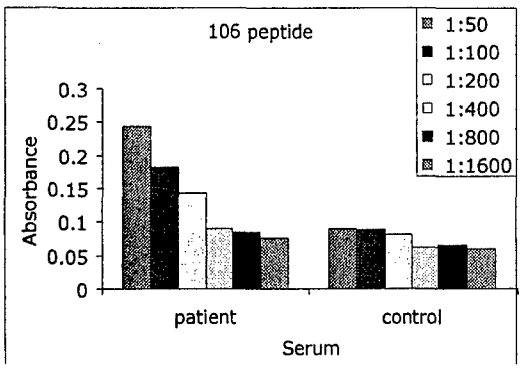

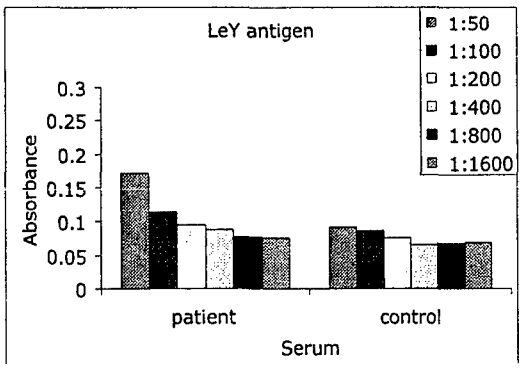

We are presently pursuing the screening of peptide 107, 106 and 105 against a human single chain antibody library to test if identified antibodies can mediate the apoptosis of tumor cells. In addition, we are examining archived tissue slides for staining with GS-1. In very preliminary studies we observed a marked restriction in GS-1 histology stains to tumor cells of breast and ovarian origin. This work is finalizing the rationale of moving forward with peptides 107 and 106 into the clinic in the coming year in Phase I.

Key research accomplishments

1. **We characterized the carbohydrate profile of 4T1 cell surface** and observed that KM-93, and GS-1 bind to 4T1 cells.
2. **We observed that transfection with Fut 3 changes the expression profile of E selectin reactivity.** Cells negatively selected for reactivity with KM93 do not express E selectin ligands. This is first time a cell line has been defined that selectively expresses P selectin ligands and opens up many avenues of research examining the properties of these ligands in a spontaneous model of metastases.
3. **We defined potential peptide mimotopes for targeting 4T1 cells in vivo.** Based on the screening of our mimotopes against the GS-1 we chose peptides that most likely mimic carbohydrate epitopes on the surface of the 4T1 cells.
4. **We observed that immunization with DNA induced IgM antibodies reactive with 4T1 cells.** The sequences of peptide mimotopes were converted to DNA and cloned in a vector that secrets coded peptides. Immunization with constructed plasmids induced IgM antibodies against Leb and leY antigen found on human breast cells, and a murine epitope found on murine 4T1 cells.
5. **We observed that DNA administration of 4T1-tumor bearing animal temporarily reduces the burden of tumor.** Mice were inoculated with tumor cells and 3-4 days after transplant therapeutic immunization was started with DNA constructs. A temporary shrinkage of tumor mass was observed in the group immunized with the construct encoding 107 peptide.
6. **DNA administration of the 107 peptide significantly increases survival rate of animals.** Survival experiments showed that immunization of tumor-bearing animals significantly increases survival rates.
7. **We observed that administration of 107 DNA inhibits liver metastases.** Two weeks after the completing of the immunization, mice were sacrificed, organs were harvested and distant-site metastases was measured by clonogenic assay.

Reportable outcome. One manuscript has been published, and two more submitted.

Manuscript published: A mimic of tumor rejection antigen associated carbohydrates mediates an anti-tumor cellular response. Behjatolah Monzavi-Karbassi, Ping Luo, Fariba Jousheghany, Marta Torres-Quiñones, Gina Cunto-Amesty, Cecile Artaud, Thomas Kieber-Emmons. Cancer Res. 2004: 64:2162-6.

Manuscript #1 submitted: Deficiency in Sialyl Lewis X Oligosaccharides promote metastasis in a mouse model of breast cancer. Behjatolah Monzavi-Karbassi, Tracy L.

Whitehead, Fariba Jousheghany, Cecile Artaud, Saeid Shaaf, Soheila Korourian, Thomas Kelly, Magda Thurin, Thomas Kieber-Emmons

Manuscript #2 submitted: Immunization with a carbohydrate mimotope results in reduction of spontaneous metastasis in an aggressive murine breast tumor model

Behjatolah Monzavi-Karbassi, Cecile Artaud, Fariba Jousheghany, Jaime Carcel-Trullols, Soheila Korourian, Thomas Kieber-Emmons

Conclusions

Defining new targets for designing novel immunotherapeutic approaches is crucial for the therapy of solid tumors. Aberrant expression of carbohydrate structures on malignant cells can be used to develop immune-based approaches for treatment. Overall in the second year of our research, we have established that:

1. Therapeutic administration of DNA format of a peptide mimotope stimulates tumor mass regression and diminishes metastasis to some organs.
2. Immune responses to mimotopes increase survival rate of tumor bearing animals.
3. In metastatic disease, carbohydrate profile of tumor surface changes, so, targeting a single antigen in an invasive metastatic cell line is not enough.

[CANCER RESEARCH 64, 2162–2166, March 15, 2004]

A Mimic of Tumor Rejection Antigen-Associated Carbohydrates Mediates an Antitumor Cellular Response

Behjatolah Monzavi-Karbassi,[1] Ping Luo,[2] Fariba Jousheghany,[1] Marta Torres-Quiñones,[2] Gina Cunto-Amesty,[2] Cecile Artaud,[1] and Thomas Kieber-Emmons[1]

[1]University of Arkansas for Medical Sciences, Little Rock, Arkansas, and [2]Department of Pathology and Laboratory Medicine, University of Pennsylvania, Philadelphia, Pennsylvania

ABSTRACT

Tumor-associated carbohydrate antigens are typically perceived as inadequate targets for generating tumor-specific cellular responses. Lectin profile reactivity and crystallographic studies demonstrate that MHC class I molecules can present to the immune system posttranslationally modified cytosolic peptides carrying O-β-linked *N*-acetylglucosamine (GlcNAc). Here we report that a peptide surrogate of GlcNAc can facilitate an *in vivo* tumor-specific cellular response to established Meth A tumors that display native O-GlcNAc glycoproteins on the tumor cell surface. Peptide immunization of tumor-bearing mice had a moderate effect on tumor regression. Inclusion of interleukin 12 in the immunization regimen stimulated complete elimination of tumor cells in all of the mice tested, whereas interleukin 12 administration alone afforded no tumor growth inhibition. Adoptive transfer of immune T cells into tumor-bearing nude mice indicates a role for CD8+ T cells in tumor regression. This work postulates that peptide mimetics of glycosylated tumor rejection antigens might be further developed for immune therapy of cancer.

INTRODUCTION

The presence of carbohydrate antigens on the surface of common human malignant tumor cells has led to studies directed toward the development of synthetic carbohydrate-based anticancer vaccines (1). Although these vaccines elicit antibody responses, it would also be advantageous if T cells could be directed to tumor-associated carbohydrate antigens (2–6). Posttranslationally modified cytosolic peptides carrying O-β-linked *N*-acetylglucosamine (GlcNAc) can be presented by class I MHC molecules to the immune system that activate CTLs, as resolved by wheat germ agglutinin (WGA)-binding profiles reacting with GlcNAc containing glycopeptides in the MHC Class I binding site (7, 8). Crystal structure analysis of T-cell receptor binding to model glycopeptides has indeed shown that T cells can recognize GlcNAc-linked glycopeptides bound by the MHC molecule (9, 10). T cells, therefore, have the potential to react with the GlcNAc moiety of glycopeptide antigens, suggesting that T cells can target to presented carbohydrate antigens on tumor cells.

In an effort to further define strategies to augment immune responses to tumor cells, we have been developing peptide mimics of tumor-associated carbohydrate antigens and have demonstrated that peptides synthesized as multivalent peptides can emulate or mimic the native clustering or presentation of tumor cell-displayed carbohydrate antigens (11). We have shown that prophylactic vaccination with a peptide surrogate, having the sequence GGIYWRYDIYWRYDIYWRYD (and referred to as peptide 106), induces a tumor-specific humoral response inhibiting tumor growth of a methylcholanthrene-induced sarcoma cell line (Meth A) *in vivo* (11). This peptide also activates an *in vitro* Meth A-specific cellular response with IFN-γ production on activation of lymphocytes with peptide (12). Characterization of the cellular response indicated that peptide-specific CD8+ T cells played an important role in mediating the tumor-specific CTL response that was inhibited by anti-Class I antibody (12).

Here, we demonstrate the ability of this peptide to stimulate the regression of established Meth A tumor in a murine model via the activation of specific antitumor cellular responses. We demonstrate that peptide 106 is a mimic of O-GlcNAc, an antigen presented on Meth A surface-expressed glycoproteins as resolved by reactivity with WGA to which the peptide also binds. Immunohistochemistry demonstrates infiltrates of lymphocytes targeting Meth A tumor cells in peptide-immunized mice and adoptive transfer of peptide-specific T cells into tumor-bearing nude mice verifies a role for CD8+ T cells in mediating tumor regression. These studies highlight a new function for peptide mimotopes of carbohydrate-associated antigens by demonstrating that they possess *in vivo* antitumor activity with CD8+ T cells as the primary effector cells.

MATERIALS AND METHODS

Mice and Tumor Inoculation. BALB/c female mice, 6–8 weeks old, were purchased from The Jackson Laboratory (Bar Harbor, ME). BALB/c nude mice (BALB/cAnNTac-*Foxn1nu* N9, *nu/nu*) were purchased from Taconic Farm Inc. (Germantown, NY). To establish tumor, each mouse was inoculated s.c. into the right flank with 5×10^5 Meth A cells (Methylcholanthrene-induced sarcoma of BALB/c origin; Ref. 11). Tumor growth was measured using a caliper and was recorded as the mean of two orthogonal diameters $[(a + b)/2]$.

Immunization. As in our previous studies (11, 12), peptide 106, having the sequence GGIYWRYDIYWRYDIYWRYD, was synthesized as a multiple-antigen peptide (Research Genetics, Huntsville, AL). Each mouse received 100 μg of 106 multiple-antigen peptide and 20 μg of QS-21 (Antigenics Inc., Framingham, MA) i.p., both resuspended in 100 μl of PBS three times at 5-day intervals. Recombinant murine interleukin (IL)-12 (Sigma, St. Louis, MO) was administered i.p. once daily for 5 days, starting on the day of the last peptide immunization.

Flow Cytometry. Acquisition and analysis were performed as described earlier (12). Cells were resuspended in a buffer containing, Dulbecco's PBS, 1% BSA, and 0.1% sodium azide and incubated with biotinylated peanut agglutinin or WGA (10 μg/ml; Vector laboratories, Burlingame, CA) for 30 min on ice. Cells were then stained with FITC-conjugated streptavidin at 1:500 dilution for another 30 min on ice.

ELISA and Inhibition Assays. ELISA was performed as described previously (11). Briefly, plates were coated with 106 multiple-antigen peptide. Biotinylated WGA was added, and binding was visualized with streptavidin-horseradish peroxidase (Sigma, St. Louis, MO). Absorbance was read, using a Bio-Tek ELISA reader (Bio-Tek instruments, Inc, Highland Park, Vermont). For inhibition assay, GlcNAc and *N*-acetylgalactosamine, attached to a polyacrylamide polymer (GlycoTech Corporation, Rockville, MA), were used as carbohydrate competitor. Biotinylated WGA (2.5 μg/ml) combined with serial concentrations of carbohydrates and incubated overnight at +4°C. Lectin/carbohydrate mix was added to the peptide-coated plates, and lectin binding was visualized by streptavidin-horseradish peroxidase as above. Mean absorbance was calculated from duplicates for

Received 5/28/03; revised 10/2/03; accepted 1/7/04.

Grant support: NIH Grant CA089480 and Department of Defense Grant DAMD17-0101-0366.

The costs of publication of this article were defrayed in part by the payment of page charges. This article must therefore be hereby marked *advertisement* in accordance with 18 U.S.C. Section 1734 solely to indicate this fact.

Requests for reprints: Thomas Kieber-Emmons, Arkansas Cancer Research Center, University of Arkansas for Medical Sciences, 4301 West Markham Street slot 824, Little Rock, AR 72205. Phone: (501) 526-5930; Fax: (501) 526-5934; E-mail: tke@uams.edu.

each carbohydrate concentration, and percentage of inhibition was calculated as: {1 − (mean of test wells/mean of control wells)} × 100.

T-Cell Purification. Splenocytes were harvested from spleens and prepared by lysis of erythrocytes and consequent washing several times with fresh medium (12). Splenocytes were first passed through nylon wool and then, using MiniMACS (Miltenyi Biotec, Auburn, CA), natural killer cells were depleted using anti-natural killer cell (DX5) microbeads. Finally, T cells were positively purified by Thy1.2-coated beads. Purified T cells were tested for purity as >97% positive for anti-CD3 antibody. For cell transfer experiments, after nylon wool passage, cells were enriched in CD4+ or CD8+ population using MiniMACS and depletion of unwanted cell populations.

IFN-γ Production by Purified T Cells. Purified T cells (1×10^6/ml) were cultured in 96-well or 24-well plates with various doses of recombinant IL-12. After 48 h of stimulation, supernatant was harvested and stored at −20 until use. Concentration of IFN-γ was measured using a quantitative ELISA kit (BioSource International Inc., Camarillo, CA) according to the manufacturer's instructions.

Adoptive Transfer of Cells. Splenocytes were collected from cured mice after tumor eradication and were used in transfer experiments. Immune splenocytes (1.5×10^7) were transferred i.p. to syngeneic nude tumor-bearing mice 7 to 10 days after inoculation of 0.5×10^6 Meth A cells into the right flank. To *in vitro* deplete CD4+ and CD8+ cells, splenocytes (1.5×10^7/each sample) were first passed through nylon wool column, and then, using MACS, we depleted CD4+ and CD8+ cells.

Histology. Tumors with surrounding tissues were excised and fixed in 10% formalin. Fixed samples were embedded in paraffin, sectioned, and stained with H&E. Sections were analyzed histologically for lymphocyte infiltration.

Statistical Analysis. Statistical analyses were performed using Student's *t* test and the χ^2 test; *P*s <0.05 were regarded as statistically significant. EXCEL and Statistica softwares were used for analyses. All of the experiments were performed at least three times.

RESULTS

Peptide Mimic of GlcNAc Moiety. It has become evident that both CD4+ and CD8+ T cells can recognize glycopeptides carrying mono- and disaccharides in a MHC-restricted manner provided the glycan group is attached to the peptide at suitable positions (13). Reactivity patterns of lectins with Meth A cells indicate that GlcNAc glycosyl epitopes are more highly expressed on Meth A tumor cells than the T antigen Galβ1–3 *N*-acetylgalactosamine epitope, because WGA displays greater reactivity with Meth A cells than peanut agglutinin (Fig. 1, *A* and *B*). WGA binds to the peptide 106 mimotope in a concentration-dependent manner as assessed by ELISA (Fig. 1*C*). This binding is selectively and significantly inhibitible by WGA-reactive GlcNAc in a concentration-dependent manner (Fig. 1*D*), further indicating that the peptide mimotope is reactive with the GlcNAc-binding site of WGA, and, therefore, peptide 106 is an effective antigenic mimic of GlcNAc.

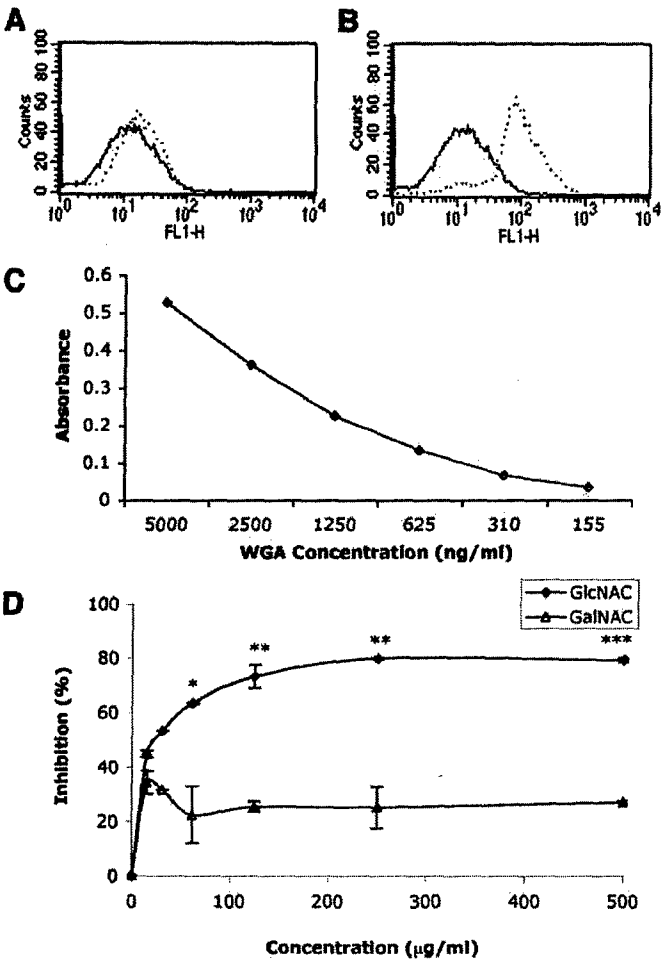

Fig. 1. Binding of wheat germ agglutinin (*WGA*) to the peptide and Meth A cells and the inhibition of WGA binding to the peptide. Meth A cells were incubated with biotinylated peanut agglutinin (*A*) or WGA (*B*) and were washed and stained with streptavidin-FITC for fluorescence-activated cell sorting (FACS) assay. Continuous and broken lines show streptavidin-FITC and lectins plus streptavidin-FITC, respectively. *C*, 96-well ELISA plates were coated with the peptide (50 μg/ml) and were incubated with biotinylated WGA; after washing, the plate binding was visualized by adding streptavidin-horseradish peroxidase. *D*, inhibition of binding of WGA to the peptide was performed by competitive carbohydrate *N*-acetylglucosamine (*GlcNAc*). *N*-acetylgalactosamine (*GalNac*) was used as a negative control. WGA was preincubated with serial dilutions of carbohydrates overnight at +4°C and then added to peptide-coated plates as above. Results present the mean value ± SD. *, $P < 0.05$; **, $P < 0.01$. ***, $P < 0.0005$, as compared with the inhibition of GalNac at the same concentration.

Therapeutic Peptide Immunization Induces Tumor Regression. To study the outcome of peptide immunization on the growth of solid tumors *in vivo*, we evaluated the antitumor effect of the peptide 106 on established Meth A tumors. BALB/c females were inoculated s.c. with Meth A cells, and 7 days later, treatment was started with the peptide. As shown in Fig. 2*A*, immunization moderately affected the growth of Meth A sarcoma, because 6 mice of 11 immunized were cured (χ^2 test, $P = 0.01$, as compared with animals that were given IL-12 only). Fig. 2*B* demonstrates that treatment of animals with IL-12 after peptide immunization tended to enhance the immune response and was successful in mediating complete eradication of established tumors (χ^2 test, $P = 0.008$, as compared with peptide-immunized only). Treatment of tumor-bearing mice with only IL-12 did not affect tumor growth (Fig. 2*C*) in keeping with other such studies (14).

We further determined that peptide/IL-12 combination therapy is highly effective even at lower doses of IL-12, because 100 ng of daily IL-12 treatment in the combined therapy, but not alone (χ^2 test, $P = 001$), eradicated tumors in five mice of five challenged (Fig. 3, *A* and *B*). The time of the beginning of immunization and the size of tumor at the time of immunization affect the efficacy of immunization. When immunizations were started at day 14 or later or when treating tumors with a mean diameter larger than 7 mm, the efficacy of immunization dropped (Fig. 3*C*), ruling out the possible effect of hyperimmunization *per se* on the outcome of the challenge experiments. To further rule out nonspecific effects of hyperimmunization, we observed that cell-based vaccination using 10^6 mitomycin-C-inactivated Meth A cells, followed by IL-12 administration, also failed to induce tumor regression (Fig. 3*D*). This latter result confirmed a previous study in which Meth A immunization along with IL-12 failed to induce tumor regression (14). Our results are in agreement with other therapeutic vaccine studies on Meth A cells, in which enhancement of antitumor T-cell responses led to quick eradication of established tumors (15, 16).

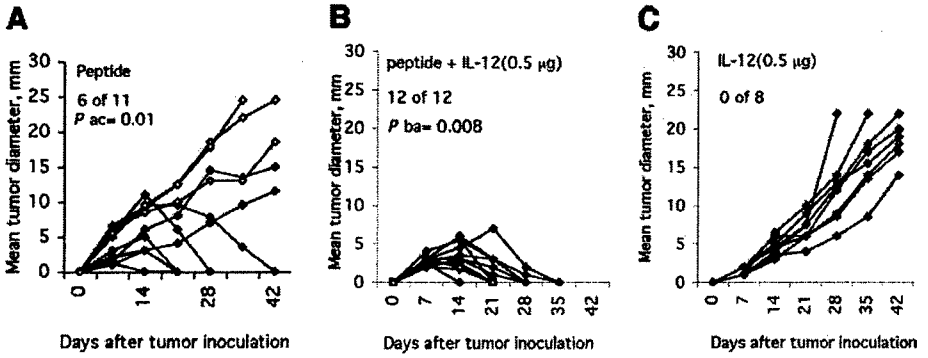

Fig. 2. Effect of peptide immunization on Meth A tumor growth and regression. BALB/c female mice were inoculated s.c. with 5×10^5 Meth A cells on day 0. *A* and *B*, 7 days after tumor inoculation peptide immunization started, mice were immunized i.p. with 106 multiple-antigen peptide/QS21 three times. Interleukin 12 was administered alone (*C*) or after peptide immunization (*B*) at indicated doses daily for 5 days, starting on the day of the last peptide immunization. Tumor growth is expressed as the mean diameter for each individual mouse. *P ac* and *P ba*, *P*s of χ^2 tests comparing *A* with *C* and *B* with *A*, respectively.

Adoptive Transfer of Splenocytes Stimulates Eradication of Tumors in Nude Mice. To further assess whether the antitumor activity mediated by peptide/IL-12 therapy is T-cell dependent, we evaluated our therapeutic strategy in nude mice. BALB/c-nu/nu mice bearing Meth A tumors were immunized with the peptide followed by IL-12 treatment. Combined peptide/IL-12 therapy had no effect on tumor growth of nude mice, indicating the dependence of mediated tumor regression on T cells (data not shown). Next, nude mice were transplanted with Meth A cells and were give injections i.p. of fresh splenocytes, isolated from cured mice, 10 days later (Fig. 4). Immune cells transferred had a dramatic effect on tumor size because by day 15 after transfer, tumor was eradicated completely in all four mice tested (χ^2 test, $P = 0.005$).

In a follow-up study, splenocytes were depleted of B cells and enriched for CD4+ or CD8+ cells, *in vitro*, and then were transferred to tumor-bearing nude mice. Our data indicate that CD8+ cells are required for efficient eradication of tumor; however, the process seems dependent on both CD4+ and CD8+ cells (Fig. 5). Histological sections of tumor sites and surrounding tissues were prepared (Fig. 6). Contrary to nonimmunized tumor-bearing mice, we detected lymphocytes around the periphery and infiltrating into tumor mass of immunized mice (Fig. 6, *A* and *B*). Staining of sections obtained from the tumor site of a cured mouse shows the presence of lymphocytes, although no tumor is detectable microscopically (Fig. 6*C*).

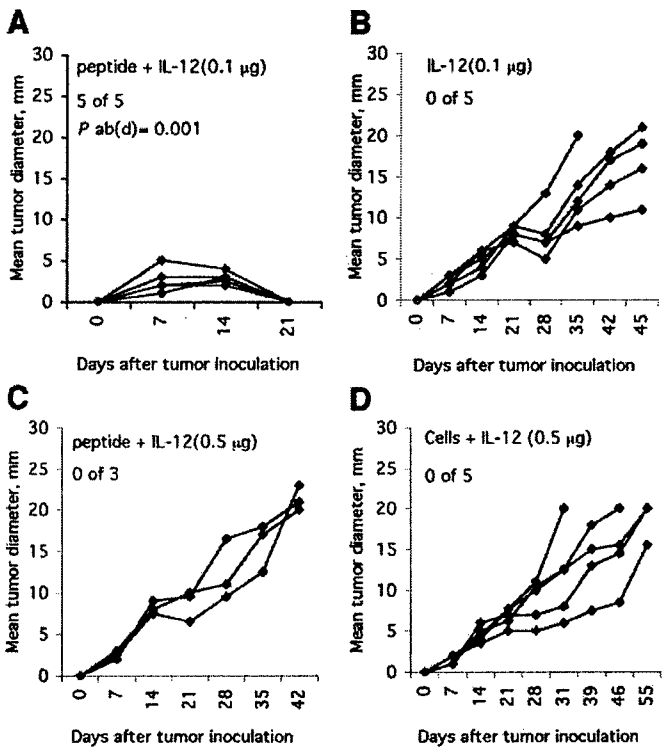

Fig. 3. Effect of late peptide or cell immunizations on the growth of the tumor. Tumor was established as explained in legend to Fig. 2. *A* and *B*, the same immunization as performed in Fig. 2 but with lower doses of interleukin (IL)-12. *C*, peptide immunization was started 14 days after tumor inoculation. *D*, 7 days after tumor inoculation, mice were immunized i.p. with 10^6 mitomycin-C-inactivated Meth A tumor cells for three times at 4–5-day intervals. IL-12 was administered alone (*B*), after peptide immunization (*A* and *C*), or after cell immunization (*D*) at indicated doses daily for 5 days, starting on the day of last peptide or cell immunization. *P ab(d)*. the *P* of χ^2 test comparing *A* with *B* or *D*.

DISCUSSION

Carbohydrates are abundantly expressed on the surface of malignant cells, and induction and enhancement of a cell-mediated immune response toward these antigens has outstanding implications in vaccination for and treatment of cancer. T-cell recognition of nonpeptidic and modified peptide antigens is, however, still poorly understood. Peptide mimetics of carbohydrate antigens can activate peptide-specific cellular responses, but they have also been shown to activate cellular responses that might be cross-reactive with carbohydrate moieties (12, 17). The induction of carbohydrate-reactive T–lymphocytes with peptide mimics is based on a functional definition of T-cell mimotopes. One possible explanation is that the peptide mimotope activates cross-reactive CTLs that recognize a processed O-linked glycopeptide associated with MHC class I. It is also possible to generate carbohydrate-specific unrestricted CTL responses with MHC class I-binding carrier peptides (18). However, we previously showed that anti-MHC Class I antibody blocks CTL killing of Meth A cells *in vitro* by T cells derived from peptide 106 immunized mice (12).

Immunization with cells in combination with IL-12 had no obvious enhancement of antitumor immune effects. Our data propose that replacing cell immunization with peptide 106 enhanced a potential immune responses resulting in a significant but moderate tumor eradication. Further treatment of peptide-immunized mice with IL-12 helped significantly in stimulating eradication of established tumor in all of the animals tested. Lack of tumor shrinkage on cell-based immunization rules out the possibility that hyperimmunization had a bearing on tumor regression. Taken together, these results indicate that peptide immunization enables an effective antitumor immune response, the potential of which can be significantly enhanced with IL-12 administration. Other groups have performed therapeutic immunization on Meth A cells by immunization with p53 mutant epitope, starting the immunizations 7 days after tumor inoculations, and have demonstrated an efficient enhancement of antitumor cellular immune responses leading to eradication of tumor mass in the majority of animals within 2 weeks after the first immunization (15, 16). Our findings are in concert with the results of these studies.

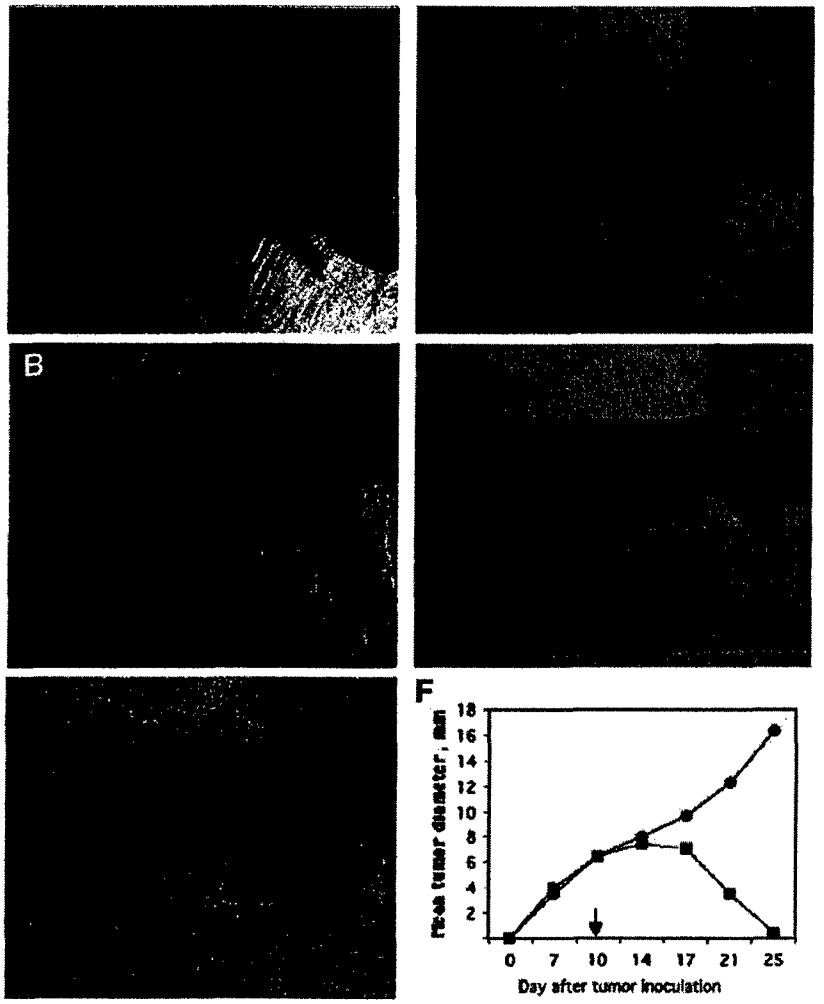

Fig. 4. Adoptive transfer of fresh immune splenocytes eradicated established tumors in nude mice. Two groups (four per group) of nude mice were inoculated s.c. with 5×10^5 Meth A cells into the right flank. Ten days after inoculation when average of tumors diameter was about 7 mm, one group was given injections i.p. of 1.5×10^7 of fresh splenocytes collected from already immunized and cured BALB/c animals. Splenocytes were prepared by lysis of erythrocytes and consequent washing several times with fresh medium. Pictures shown are taken from a representative individual on the day of cell transfer (*A*), 7 days later (*B*), 12 days later (*C*), and 17 days later (*D*). *E*, tumor size in control group 25 days after transplant as one representative individual of four is shown. *F*, average of tumor diameter for four mice per group in naïve control (●) and splenocyte-transferred groups (■). *Arrow*, the date of injection of splenocytes.

Because resting T cells do not express the IL-12 receptor (19) and IL-12 responsiveness is only activated after T-cell receptor stimulation (20), we observed that purified peptide-specific T cells were stimulated with IL-12 *in vitro* (data not shown). IL-12 treatment is ineffective in the Meth A tumor model (14) as further observed in our studies. Because IL-12 responsiveness of T cells is induced after T-cell receptor stimulation, the lack of IL-12 responsiveness suggests that T cells in Meth A-bearing mice are not sensitized to Meth A tumor antigen on immunization with Meth A cells. In contrast, our data suggest that peptide immunization can sensitize tumor-reactive T cells that are responsive to IL-12. It is possible that peptide immunization further expands B and T cells that have been primed via shed glycoprotein(s) processing. We propose that peptide 106 immunization activated a population of Th1 and CTLs with production of IFNγ (12), and *in vivo* IL-12 treatment further helps to expand the T-cell population and IFNγ production. In previous studies, the failure of IL-12 treatment to induce tumor regression was also considered to be associated with the lack of T-cell migration to tumor sites (14). It was argued that sensitization of T cells to tumor antigens and generation of IL-12 responsiveness are insufficient to induce tumor regression when sensitized T cells are not allowed to migrate to tumor sites. In our studies, we observe lymphocyte migration to tumor sites.

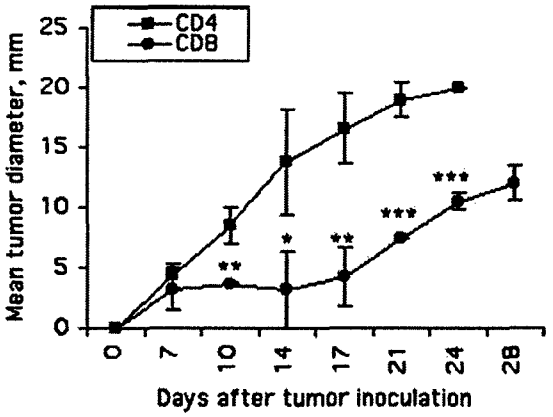

Fig. 5. CD8+ T cells are required for successful adoptive therapy of established tumors. Solid tumors were established in nude mice, and at day 7, enriched splenocytes were transferred i.p. For enrichment, splenocytes were passed through nylon wool after which the percentage of CD19+ cells that remained were less than 7%. The percentage of CD8+ and CD4+ cells in CD4 and CD8-enriched population was less than 10%. Results present the mean value ± SD. *, $P < 0.05$; **, $P < 0.01$. ***, $P < 0.0005$, as compared with mean tumor diameter of CD4+ -transferred animals.

In summary, this work further postulates the occurrence of saccharide epitopes for T cells linked to peptides with anchoring motifs for MHC Class I (6, 13). Although analogous to the haptens trinitrophenyl and O-β-linked acetyl-glucosamine, the potential implications of natural carbohydrates as antigenic epitopes for CTL in biology are considerable and are understudied. Consequently, it might be possible for peptide mimetics to activate T cells that recognize carbohydrate moieties on native glycopeptides (21). Peptides that mimic carbohydrate structures attached to class I or class II anchoring peptides would

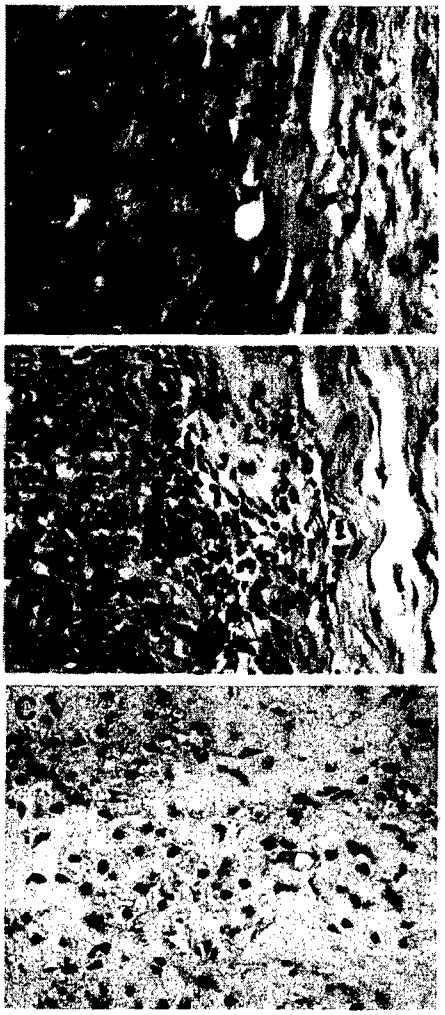

Fig. 6. Lymphocytes infiltrate the Meth A challenge site in immunized mice. Fixed sections from tumor site of nonimmunized tumor-bearing mice (*A*), immunized tumor-shrinking mice (*B*), and immunized tumor-eliminated mice (*C*) stained with H&E. Mice were transplanted, and immunization started 7 days later. Samples were obtained when tumor was 16 mm (*A*) and 2 mm (*B*) and at 5 days after tumor eradication (*C*).

extend our notion of vaccine design for cancer immunotherapy in the adjuvant setting.

ACKNOWLEDGMENTS

We thank Charlotte Read Kensil of Antigenics Inc. (Framingham, MA) for the QS-21. We thank Eric Siegel of the department of Biometry, University of Arkansas for Medical Sciences, for advise on the statistical analysis.

REFERENCES

1. Danishefsky SJ, Allen JR. From the laboratory to the clinic: a retrospective on fully synthetic carbohydrate-based anticancer vaccines [frequently used abbreviations are listed in the appendix]. Angew Chem Int Ed Engl 2000;39:836–63.
2. Jensen T, Galli SL, Mouritsen S, et al. T cell recognition of Tn-glycosylated peptide antigens. Eur J Immunol 1996;26:1342–9.
3. Jensen T, Hansen P, Galli SL, et al. Carbohydrate and peptide specificity of MHC class II-restricted T cell hybridomas raised against an O-glycosylated self peptide. J Immunol 1997;158:3769–78.
4. Haurum JS, Arsequell G, Lellouch AC, et al. Recognition of carbohydrate by major histocompatibility complex class I-restricted, glycopeptide-specific cytotoxic T lymphocytes. J Exp Med 1994;180:739–44.
5. Galli-Stampino L, Meinjohanns E, Frische K, et al. T-cell recognition of tumor-associated carbohydrates: the nature of the glycan moiety plays a decisive role in determining glycopeptide immunogenicity. Cancer Res 1997;57:3214–22.
6. Zhao XJ, Cheung NK. GD2 oligosaccharide: target for cytotoxic T lymphocytes. J Exp Med 1995;182:67–74.
7. Haurum JS, Hoier IB, Arsequell G, et al. Presentation of cytosolic glycosylated peptides by human class I major histocompatibility complex molecules in vivo. J Exp Med 1999;190:145–50.
8. Kastrup, IB, Stevanovic, S, Arsequell, G, et al. Lectin purified human class I MHC-derived peptides: evidence for presentation of glycopeptides in vivo. Tissue Antigens 2000;56:129–35.
9. Glithero A, Tormo J, Haurum JS, et al. Crystal structures of two H-2Db/glycopeptide complexes suggest a molecular basis for CTL cross-reactivity. Immunity 1999;10: 63–74.
10. Speir JA, Abdel-Motal UM, Jondal M, Wilson IA. Crystal structure of an MHC class I presented glycopeptide that generates carbohydrate-specific CTL. Immunity 1999; 10:51–61.
11. Kieber-Emmons T, Luo P, Qiu J, et al. Vaccination with carbohydrate peptide mimotopes promotes anti-tumor responses. Nat Biotechnol 1999;17:660–5.
12. Monzavi-Karbassi B, Cunto-Amesty G, Luo P, Shamloo S, Blaszcyk-Thurin M, Kieber-Emmons T. Immunization with a carbohydrate mimicking peptide augments tumor-specific cellular responses. Int Immunol 2001;13:1361–71.
13. Werdelin O, Meldal M, Jensen T. Processing of glycans on glycoprotein and glycopeptide antigens in antigen-presenting cells. Proc Natl Acad Sci USA 2002;99: 9611–3.
14. Gao P, Uekusa Y, Nakajima C, et al. Tumor vaccination that enhances antitumor T-cell responses does not inhibit the growth of established tumors even in combination with interleukin-12 treatment: the importance of inducing intratumoral T-cell migration. J Immunother 2000;23:643–53.
15. Noguchi Y, Richards EC, Chen YT, Old LJ. Influence of interleukin 12 on p53 peptide vaccination against established Meth A sarcoma. Proc Natl Acad Sci USA 1995;92:2219–23.
16. Mayordomo JI, Loftus DJ, Sakamoto H, et al. Therapy of murine tumors with p53 wild-type and mutant sequence peptide-based vaccines. J Exp Med 1996;183: 1357–65.
17. Tzianabos AO, Finberg RW, Wang Y, et al. T cells activated by zwitterionic molecules prevent abscesses induced by pathogenic bacteria. J Biol Chem 2000;275: 6733–40.
18. Abdel-Motal U, Berg L, Rosen A, et al. Immunization with glycosylated Kb-binding peptides generates carbohydrate-specific, unrestricted cytotoxic T cells. Eur J Immunol 1996;26:544–51.
19. Desai BB, Quinn PM, Wolitzky AG, Mongini PK, Chizzonite R, Gately MK. IL-12 receptor. II. Distribution and regulation of receptor expression J Immunol 1992;148: 3125–32.
20. Maruo S, Toyo-oka K, Oh-hora M, et al. IL-12 produced by antigen-presenting cells induces IL-2-independent proliferation of T helper cell clones. J Immunol 1996;156: 1748–55.
21. Sandmaier BM, Oparin DV, Holmberg LA, Reddish MA, MacLean GD, Longenecker BM. Evidence of a cellular immune response against sialyl-Tn in breast and ovarian cancer patients after high-dose chemotherapy, stem cell rescue, and immunization with Theratope STn-KLH cancer vaccine. J Immunother 1999;22:54–66.